

# Relationship between Pore Occupancy and Gating in BK Potassium Channels

Rebecca A. Piskorowski and Richard W. Aldrich

Section of Neurobiology, University of Texas at Austin, Austin, TX 78712

Permeant ions can have significant effects on ion channel conformational changes. To further understand the relationship between ion occupancy and gating conformational changes, we have studied macroscopic and single-channel gating of BK potassium channels with different permeant monovalent cations. While the slopes of the conductance–voltage curve were reduced with respect to potassium for all permeant ions, BK channels required stronger depolarization to open only when thallium was the permeant ion. Thallium also slowed the activation and deactivation kinetics. Both the change in kinetics and the shift in the GV curve were dependent on the thallium passing through the permeation pathway, as well as on the concentration of thallium. There was a decrease in the mean open time and an increase in the number of short flicker closing events with thallium as the permeating ion. Mean closed durations were unaffected. Application of previously established allosteric gating models indicated that thallium specifically alters the opening and closing transition of the channel and does not alter the calcium activation or voltage activation pathways. Addition of a closed flicker state into the allosteric model can account for the effect of thallium on gating. Consideration of the thallium concentration dependence of the gating effects suggests that the flicker state may correspond to the collapsed selectivity filter seen in crystal structures of the KcsA potassium channel under the condition of low permeant ion concentration.

## INTRODUCTION

The permeation and gating processes of ion channels are frequently treated as two independent processes. However, there is increasing evidence to support the idea that the selectivity filter may play a role in the gating conformational changes of potassium channels. This evidence comes from four classes of results. First, mutations near or in the selectivity filter of several potassium channels have been found to alter permeation and gating. Backbone mutations in the selectivity filter (the key amide carbonyls in the selectivity filter were changed to ester carbonyls) of  $K_{IR}2.1$  were found to have significant effects on gating (Lu et al., 2001a). In *Shaker* channels, a mutation near the selectivity filter, T442S, was found to induce subconductance levels that were coupled to activation (Zheng and Sigworth, 1998). The mutation Y293W in BK channels was found to decrease the open time in single channel records for inward currents only (Lagrutta et al., 1998). Neutralization of a neighboring residue in BK channels, D292N, had major effects on the biophysical properties of the channel (Haug et al., 2004b). These results strongly suggest that the selectivity filter dynamics can alter the gating processes of potassium channels.

Second, changes in gating have been observed for potassium channels in the presence of external ions such as rubidium and cesium. Specifically, the deactivation

rate is reduced with external rubidium and cesium (Swenson and Armstrong, 1981; Clay and Shlesinger, 1983, 1984; Matteson and Swenson, 1986). Barium block at certain sites in the BK channel selectivity filter altered gating (Neyton and Miller, 1988a,b) (Neyton and Pelleschi, 1991). Demo and Yellen (1992) found that external rubidium and cesium were able to slow the deactivation and increase the activation rate of BK channels. In this case, occupancy of the same site in the selectivity filter by rubidium or cesium prohibited channel closing (Demo and Yellen, 1992). Changes in the single channel kinetics with rubidium and thallium have been reported for several different potassium channels. Rubidium has consistently been reported to increase the open dwell time of BK (Demo and Yellen, 1992; Mienville and Clay, 1996, 1997), KcsA (LeMasurier et al., 2001), KCNQ1 (Pusch et al., 2000), ROMK2 (Choe et al., 2001), and IRK1 channels (Choe et al., 2001). On the other hand, thallium has been found to consistently reduce the open dwell times for several potassium channels: BK (Blatz and Magleby, 1984), KcsA (LeMasurier et al., 2001), ROMK2 (Chepilko et al., 1995; Choe et al., 2001; Lu et al., 2001b), and IRK1 (Choe et al., 2001).

Third, several experiments have demonstrated that occupancy in the selectivity filter of  $K_V$  channels can influence on-gating charge movement and activation (Consiglio et al., 2003; Consiglio and Korn, 2004), as well

Correspondence to Richard W. Aldrich: raldrich@mail.utexas.edu

R.A. Piskorowski's present address is Department of Physiology, University of California at San Francisco, San Francisco, CA 94107.

Abbreviation used in this paper: NMG, *N*-methyl glucamine.

TABLE I  
Model Parameters of Scheme 1

$P_o = \frac{L(1 + KC + JD + JKCDE)^4}{L(1 + KC + JD + JKCDE)^4 + (1 + J + K + JKE)^4}$	The allosteric model of Scheme 1 can account for the steady-state properties BK channel gating with three equilibrium constants ( $L$ , $J$ , and $K$ ) and three allosteric factors ( $C$ , $D$ , and $E$ ) (Horrigan and Aldrich 2002).
$L = L_0 \exp\left(\frac{QV}{kT}\right)$	$L$ is the closed to open equilibrium constant, with $L_0$ as the zero voltage value of $L$ , and $Q$ as the partial charge of the conformational change between the closed and open state.
$J = J_0 \exp\left(-\frac{zV}{kT}\right)$	$J$ is the voltage sensor equilibrium constant with $J_0$ as the zero voltage value of $J$ , and $z$ as the partial charge of the voltage sensor.
$K = \frac{[Ca^{2+}]}{K_D}$	$K$ is the equilibrium constant for calcium binding with $K_D$ as the $Ca^{2+}$ dissociation constant of the closed state.
$D = \frac{e^{-\frac{zV_{hC}}{kT}}}{e^{-\frac{zV_{hO}}{kT}}}$	$D$ is the allosteric factor describing interactions between channel opening and voltage sensor activation with $z$ as the partial charge of the voltage sensor, and $V_{hC}$ and $V_{hO}$ as the half activation voltages of the closed and open states, respectively.
$C = \frac{K_C}{K_O}$	$C$ is the allosteric factor describing interactions between channel opening and $Ca^{2+}$ binding with $K_C$ and $K_O$ as the $Ca^{2+}$ dissociation constant for the closed and open channel, respectively.
$E$	$E$ is the allosteric factor describing interactions between $Ca^{2+}$ binding and voltage sensor activation.

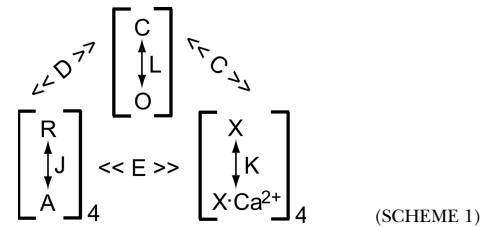
as the rate of off-gating charge movement and deactivation (Chen et al., 1997; Hurst et al., 1997; Wang et al., 1999). Consiglio and Korn (2004) propose that the outer vestibule of the selectivity filter is in close proximity to the S4 voltage sensor and that structural perturbations of the selectivity filter by ion occupancy can affect voltage-sensing motions of the S4. In the absence of all internal and external potassium ions, *Shaker* channels were found to enter a stable, noninactivating, nonconducting conformation called the “defunct state” (Gomez-Lagunas, 1997; Melishchuk et al., 1998; Loboda et al., 2001).

Lastly, permeant ions and occupancy in the selectivity filter have been found to affect C-type inactivation in several voltage-gated potassium channels. Increasing the occupancy of the selectivity filter with external potassium or blocking ions decreased the rate of C type inactivation for *Shaker* and Kv channels (Lopez-Barneo et al., 1993; Baukrowitz and Yellen, 1995, 1996; Harris et al., 1998; Kiss and Korn, 1998; Kiss et al., 1999). Point mutations near the selectivity filter indirectly altered C type inactivation rates by reducing the occupancy of the selectivity filter (Ogielska and Aldrich, 1998, 1999).

Recent crystallographic results have revealed how the low  $K^+$  form of the crystal structure depends on the identity of the permeating ion (Zhou and MacKinnon, 2003). In these experiments, the KcsA structure was solved with different concentrations of potassium or thallium. The selectivity filter was found to adopt the same collapsed structure in low thallium or low potassium concentrations. The filter was found to switch sharply from the collapsed structure to the conducting

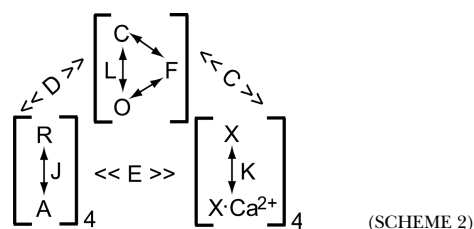
structure at  $\sim 20$  mM potassium or at  $\sim 80$  mM thallium (Zhou and MacKinnon, 2003). This persistence of the collapsed structure in the presence of higher concentrations of thallium indicates that thallium is not as effective as potassium at stabilizing the conducting structure.

BK channels have been extensively studied at the single channel and macroscopic levels. An allosteric model has been developed by Horrigan et al. (Horrigan and Aldrich, 1999, 2002; Horrigan et al., 1999) that can describe channel gating over a very wide range of calcium concentrations and voltages while also providing mechanistic insight into channel gating (Scheme 1 and Table I). However, even such detailed allosteric models are oversimplifications of channel gating. They do not account for short flicker closing events observed in the single channel data (Cox et al. 1997, Rothberg and Magleby 1998; Horrigan and Aldrich, 2002) or for the effect of permeating ions on channel gating.



We have examined the gating properties of BK channels with different permeant ions to further understand the interactions between occupancy and gating. The allosteric

model presented in Scheme 1 was applied to determine which aspects of BK channel gating were being altered by the permeant ion. The macroscopic and single channel kinetics in thallium solutions could both be accounted for by the addition of a short-lived nonconducting flicker state (Scheme 2). This flicker state may be related to the collapsed structure of the selectivity filter seen with KcsA.



## MATERIALS AND METHODS

### Channel Expression

The wild-type BK channel construct used in these experiments was the *mbr5* clone of the mouse *mslo* gene, which was provided by L. Salkoff (Washington University School of Medicine, St. Louis, MO). Several silent mutations were made throughout this clone to facilitate subcloning and mutagenesis. The *mBr5* clone was propagated in a modified Blue Script vector BS-MXT (Stratagene) in the *Escherichia coli* strain DH5- $\alpha$ . cRNA was transcribed from this vector in vitro using the mMessage mMachine kit with T3 polymerase (Ambion). For macroscopic recordings,  $\sim 0.05$ – $0.5$  ng of cRNA was injected into *Xenopus laevis* oocytes 2–8 d before recording. *mBr5* was also incorporated into a mammalian expression vector containing the SV-40 promoter. HEK293 cells expressing the large T-antigen of the SV-40 virus promoter were cotransfected with *mBr5* and a transcript encoding green fluorescent protein was used as a transfection marker. Approximately  $1 \mu\text{g}$  DNA was transfected onto plates using Lipofectamine 2000 (Invitrogen).

### Electrophysiology

Excised patches, in inside-out and outside-out configurations, were transferred into a separate chamber and washed with at least 50 volumes of internal solution. All experiments were done at  $22^\circ\text{C}$ . Patches were allowed to stabilize for at least 5–10 min before recording. K currents were recorded with internal solutions containing (in mM) 100 mM  $\text{KNO}_3$ , 20 mM HEPES, 4 HCl and 40  $\mu\text{M}$  (+)-18-crown-6-tetracarboxylic acid (18C6TA) to chelate contaminating barium. “0 calcium” solutions contained 5 mM EGTA, reducing free calcium to  $\sim 0.8$  nM. Calcium solutions were buffered with HEDTA, EGTA, or NTA, depending on the targeted free concentration. Calcium concentrations were measured with a calcium electrode (Orion Research, Inc.). External potassium solutions contained (in mM) 100  $\text{KNO}_3$ , 20 HEPES, and 2  $\text{MgCl}_2$ . The pH for the internal and external solutions was adjusted to 7.2 with methane sulfonic acid (MES). For thallium solutions,  $\text{KNO}_3$  was replaced in all solutions by  $\text{TlNO}_3$ .  $\text{TlOH}$  was added to account for the difference in activity between  $\text{KNO}_3$  and  $\text{TlNO}_3$ . For *N*-methyl glucamine (NMG) and sucrose solutions, 100 mM *N*-methyl glucamine-methane sulfonate replaced  $\text{KNO}_3$ , 200 mM sucrose replaced  $\text{KNO}_3$ . Extreme care was taken to account for all junction potential errors. Junction potentials were measured for all possible solution configurations, and the data were adjusted accordingly. There was never any junction potential error  $> 7$  mV.

Data were acquired at room temperature with an Axon 200-A patch clamp amplifier (Axon Instruments, Inc.) in the resistive

feedback mode and a Macintosh-based computer system using Pulse acquisition software (HEKA Elektronik) and the ITC-16 hardware interface (Instrutech Scientific Instruments). Unless otherwise indicated, currents were digitized at 20- $\mu\text{s}$  intervals for macroscopic currents and 5- $\mu\text{s}$  intervals for single channel currents. Experiments were low-pass filtered at 20 kHz using an external eight pole Bessel filter (Frequency Devices). Before macroscopic currents were analyzed, capacity and leak currents were subtracted using a P/5 leak subtraction protocol with a holding potential of  $-120$  mV and voltage steps opposite in polarity to those in the experimental protocol. Patch pipettes were made with borosilicate glass (VWR Micropipettes) or thick walled 1010 glass (World Precision Instruments), coated with wax (KERR sticky wax) to minimize electrode capacitance and fire polished before being used. Pipette access resistance was measured in bath solutions (0.5–1.5  $\text{M}\Omega$ ). For recordings with currents  $> 2$  nA, the internal circuitry of the amplifier was used to compensate for at least 80% of the series resistance. For recordings with  $< 2$  nA of current, the pipette access resistance was used to estimate the series resistance errors of the command voltage and corrections to this error were made to the command potential. For all kinetic measurements, there was  $< 5$  mV series resistance error.

Data were analyzed using Igor Pro software (WaveMetrics) and single channel data were analyzed using the ScanApp analysis software developed by Dorothy Perkins and Dan Cox.

To record the GV curves, patches were held at  $-100$  mV and then stepped to from  $-100$  to  $140$  mV at 10-mV intervals for 20 ms and then stepped down to  $-80$  mV. To increase the signal to noise ratio, 4–12 current families were recorded under identical conditions and averaged before display and analysis. The minimal inward current during the  $-80$  mV voltage step (i.e., the “tail” current) was plotted as a function of the voltage of the preceding step. The normalized plot of these values is a measure of the channel’s ability to open over a range of voltages. GV curves were fit with a Boltzmann function:  $G = \{1 + \exp[-z(V - V_{1/2})/kT]\}^{-1}$ .

The deactivation kinetics were measured by holding the membrane potential at 150 mV for 30 ms to open all of the channels and then stepping to a series of potentials (from  $-200$  to  $+200$  mV) at which the deactivation time constant was measured by a single exponential fit. The deactivation currents were fit with single order exponentials and the goodness of fit was evaluated. Near the reversal potential, fits were performed on small currents; the small size of the current created some variability in the fits. However, this variability was reduced when the deactivation rates from multiple patches were averaged ( $n = 13$ – $17$ ).

## RESULTS

### Effects of Permeant Monovalent Cations on BK Channel Gating

Macroscopic BK channel currents were recorded in symmetrical solutions of potassium, rubidium, cesium, and thallium (Fig. 1 A). As previously described, changes in gating kinetics were observed with rubidium and cesium (Demo and Yellen, 1992). Rubidium and cesium both increased the activation rate and decreased the deactivation rate. For currents recorded in rubidium and cesium, there was no significant change in the range of voltages required to open the channel, as illustrated by the conductance versus voltage curve (Fig. 1 B).

Symmetrical thallium ions were found to have a dramatic effect on the range of voltages at which the channels open (Fig. 1 B), shifting the GV curve by approximately

+38 mV. Fig. 1 (C and D) shows paired current traces from patches recorded with either symmetrical potassium or symmetrical thallium. Thallium slows the activation and deactivation of BK channels.

#### Permeating Thallium Alters Channel Kinetics

The effects of symmetrical thallium on gating could arise from either thallium occupancy of the pore, an action of thallium at an internal or external site on the channel protein, or both. If thallium is acting on the channel as it passes through the permeation pathway, it would be predicted that the kinetics would only be altered when thallium is primarily occupying the selectivity filter. The selectivity filter can be selectively occupied by controlling the internal solution and the direction of the current.

The deactivation kinetics were measured under four conditions: symmetrical thallium, symmetrical potassium, internal potassium with external thallium, and internal thallium with external potassium. The deactivation kinetics displayed a dramatic dependence on the direction of current flow. A plot of the deactivation time constants as a function of voltage for data with internal potassium is shown in Fig. 2 A with either external potassium or external thallium. At positive potentials, potassium was the permeating ion and primarily occupied the selectivity filter. At these voltages, the deactivation rate constants were not affected by the external thallium and corresponded to the deactivation rate seen in symmetrical potassium. At negative potentials, current was flowing from the external side of the membrane to the internal side. The deactivation rate constants from currents recorded with external thallium abruptly shifted at the reversal potential, reflecting the slower kinetics induced by thallium. At negative potentials, a difference was seen in the rate constants between inward potassium currents and inward thallium currents. The same dependence on deactivation rate with permeating ion was seen with internal thallium and external thallium or potassium (Fig. 2 B). At positive potentials above the reversal potential, the outward current corresponds to the slower thallium deactivation time constants. The kinetics with external potassium abruptly shifted at the reversal potential to slower deactivation rates as internal thallium primarily occupied the selectivity filter. Taken together, these results argue strongly that the effects of thallium on tail current kinetics occur as a result of thallium occupancy in the channel.

The abrupt change in kinetics at the reversal potential suggests that the selectivity filter undergoes a surprisingly steeply voltage-dependent change of occupancy at the reversal potential. Such a steep voltage dependence of occupancy is compatible with the high conductance and well-documented ion-ion interactions in BK channels. Strong ion interactions would lead to a large flux-ratio exponent (Hille, 2001), which would be

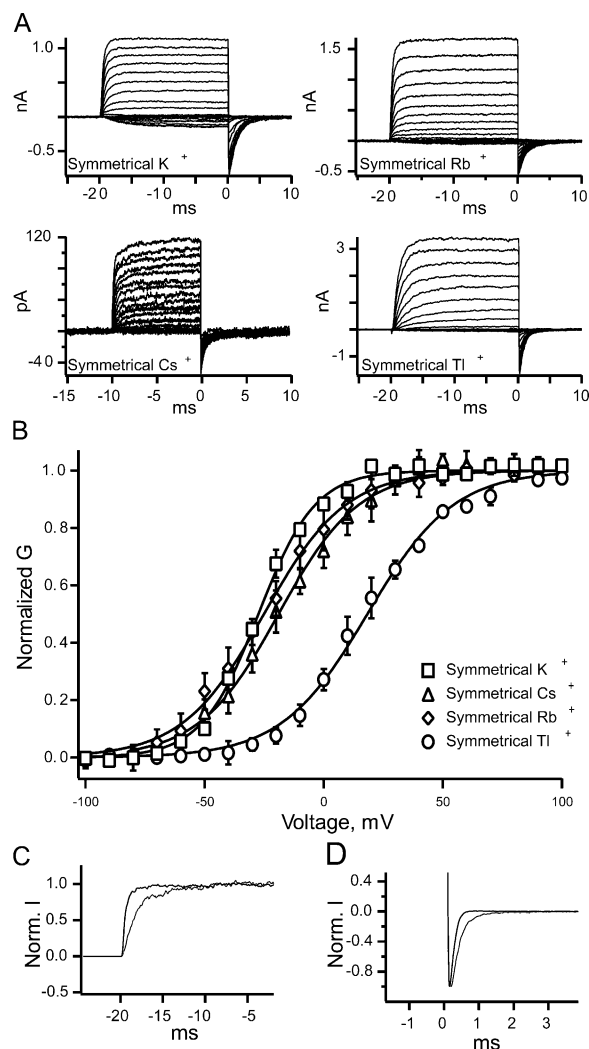


**Figure 1.** BK channel currents recorded with four different permeant ions. (A) Currents recorded with 100 mM symmetrical potassium, rubidium, cesium, and thallium. (B) The conductance versus voltage curve from currents recorded in symmetrical potassium (squares), symmetrical cesium (triangles), symmetrical rubidium (diamonds), and symmetrical thallium (circles). Thallium produced a significant shift in the GV curve to higher potentials as analyzed by a shift in the  $V_{1/2}$  of the Boltzmann fit (by ANOVA,  $P = 6.87 \times 10^{-8}$ ), unlike cesium and rubidium ( $P = 0.845$  for cesium and  $P = 0.954$  for rubidium). Thallium, rubidium, and cesium all changed the slope of the GV curve. Thallium alters the gating of BK channels: (C) Currents in response to a 200-mV voltage step traces recorded from the same patch. Currents were normalized to the maximal steady-state current for both symmetrical potassium (black) and symmetrical thallium (gray). (D) Inward tail currents in response to a  $-80$ -mV pulse. These currents were preceded by a  $+200$ -mV pulse. Currents are normalized to the peak of the tail current. Solutions are either symmetrical potassium (black) or symmetrical thallium (gray). All currents were recorded with  $300 \mu\text{M}$  internal calcium.

expected to tightly correlate the unidirectional fluxes and net fluxes, causing a steep voltage dependence to the change in the directionality of the net flux at the reversal potential.

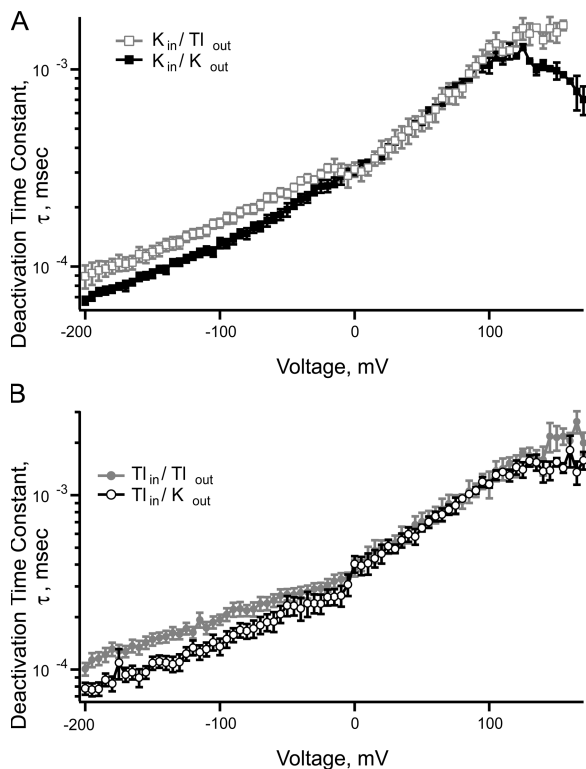


**Figure 2.** Deactivation rates shift at the reversal potential under biionic conditions. (A) Deactivation rates from data collected in symmetrical potassium (solid black squares) or internal potassium with external thallium (open gray squares). (B) Deactivation rates from data collected in symmetrical thallium (solid gray circles) or internal thallium with external potassium (open black circles). Each data point is the mean  $\pm$  SEM. For symmetrical potassium,  $n = 19$ , symmetrical thallium,  $n = 17$ , internal thallium with external potassium,  $n = 15$ , internal potassium with external thallium,  $n = 13$ . Zero internal calcium.

### Effects of Thallium on Steady-state Gating

As shown in Fig. 1, thallium shifts the range of voltages required to open the channel to higher potentials. Is this effect on the steady-state kinetics due to thallium interacting through the selectivity filter or somewhere else in the channel?

To address this question, currents were recorded under two biionic conditions: external potassium with internal thallium and external thallium with internal potassium. If thallium can only alter the GV from one side of the membrane, and not via the permeation pathway, then a shift in the GV curve would be expected for only one of these conditions. If thallium is shifting the GV by a site on the external face of the channel, a shift in the GV would be seen only in conditions containing external thallium.

The GV shifted relative to symmetrical potassium for both biionic conditions. As shown in Fig. 3, the  $V_{1/2}$  for symmetrical potassium was  $-29.8 \pm 8.657$  mV ( $n = 29$ ), for internal potassium with external thallium it was  $-7.01 \pm 8.52$  mV ( $n = 15$ ), and for internal thallium with external potassium it was  $-0.09 \pm 6.3$  mV ( $n = 17$ ).

For symmetrical thallium, the  $V_{1/2}$  was  $3.75 \pm 7.49$  mV ( $n = 21$ ). If thallium is acting on the channel through the permeation pathway alone, then the ion carrying the current will dictate the gating behavior of the channel. Since the GV curves for the two biionic solutions straddle the reversal potential, potassium and thallium would both carry the current at voltages where the GV curve is determined. This would potentially create a smaller shift in the GV than if thallium alone were permeating.

The GV shift by thallium was further analyzed under conditions in which only one kind of ion is passing through the selectivity filter. A consistent change in the slope ( $z$ ) of the GV curve is seen along with its shift to more positive voltages. This effect of thallium depends on the sidedness of thallium action. This slope of the GV curve was  $1.31 \pm 0.27$  ( $n = 17$ ) for internal potassium with external thallium and  $1.79 \pm 0.15$  ( $n = 15$ ) for internal thallium with external potassium.

A series of experiments was performed with the non permeant ion NMG in order to assess the effect of the charge carrying ion on the GV curve. All of the permeant ions on one side of the membrane were replaced with NMG. Conditions were selected so that all currents would only be going through the membrane in one direction over the range of activation voltages. For example, to investigate how the internal ion alters gating in the BK channel, all external permeant ions were replaced by NMG, and the internal calcium concentration was lowered to  $2 \mu\text{M}$  so that the channels would require more positive voltages to activate. The patches were stepped from 0 to 210 mV and the tails were recorded at 5 mV. Under these conditions, the selectivity filter could only be populated by the internal ion.

Fig. 4 (A and B) shows data from patches recorded with external NMG and either internal potassium or thallium solutions. Internal thallium shifted the GV curve by  $\sim 33$  mV relative to internal potassium. While the shift in the GV curve was similar to the shift seen with symmetrical solutions ( $\sim 30$  mV), the slope of the GV was found not to significantly differ between conditions with internal potassium ( $z = 1.84 \pm 0.07$ ,  $n = 5$ ) and internal thallium ( $z = 1.85 \pm 0.02$ ,  $n = 6$ ) by ANOVA,  $P = 0.9993$ . These results indicate that thallium is acting on the channel via the permeation pathway or the internal face of the channel to shift the  $V_{1/2}$ . The change in slope seen with symmetrical and external thallium/internal potassium solutions seems to be due to an interaction between thallium and an external site.

To investigate any potential interactions between thallium and the external face of the channel, the opposite NMG experiment was performed. All of the internal permeant ions were replaced by NMG, and either thallium or potassium solutions were external. The internal calcium concentration was raised to  $300 \mu\text{M}$  so the channels would be active at negative voltages below the reversal potential. As shown in Fig. 4 (F and G), the GV

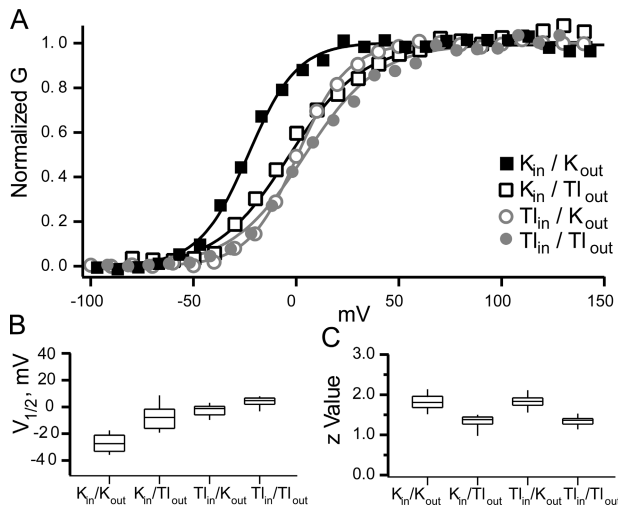


**Figure 3.** The gating of BK channels is influenced differently by internal and external thallium solutions. (A) The GV curve of BK channels recorded in four conditions: symmetrical potassium (solid black squares), internal potassium with external thallium (open black squares), internal thallium with external potassium (open gray circles), and symmetrical thallium (closed gray circles). The solid lines are fits with Boltzmann curve. (B) Box plots of the half activation,  $V_{1/2}$ , from the Boltzmann fits for the four conditions. (C) Box plots of the  $z$  values from the Boltzmann fits. Box plots display the median and the 10th, 25th, 75th, and 90th percentiles. All data was recorded in 300  $\mu\text{M}$  internal calcium.

was shifted by  $\sim 38$  mV. This shift indicates that thallium does not need to interact with the intracellular face of the channel to induce the GV curve shift. However, the shift in  $V_{1/2}$  from external ions flowing inward is compounded by a reduction in the slope of the GV curve. For external potassium, the  $z$  value was  $1.4 \pm 0.11$ , and for external thallium it was  $1.1 \pm 0.10$ . The shift in the  $V_{1/2}$  is larger for this set of conditions than when thallium carried outward current, and it is likely due to this additional effect of external thallium on the GV curve's slope along with the effect of the thallium and the permeation pathway.

The slopes from the GV curves of currents recorded with internal NMG solutions were shallower than the slope from currents recorded with internal permeant ions ( $1.4 \pm 0.16$  for symmetrical thallium and  $1.84 \pm 0.27$  for symmetrical potassium). Extra care was taken to correct for any artifacts arising from nonconducting solutions (junction potential shifts, series resistance). However, it is possible that this change in slope may be a result of complications from the absence of permeant ions on one side of the membrane. NMG has been shown to compete with potassium for a site in the internal vestibule (Lippiat et al., 1998); therefore NMG may have an unpredictable effect on pore occupancy under these conditions. To rule out a specific effect of NMG on the permeation pathway, these experiments were repeated with internal sucrose. The reduction in the GV curve slope was similar with internal NMG or sucrose.

From these results, it can be concluded that thallium can shift the GV curve to more positive voltages from either side of the membrane. In addition, external thallium causes the GV curve to be shallower. This reduction in slope contributes to the larger  $V_{1/2}$  shift observed in conditions with external thallium. Thallium has two different effects on BK channel gating: one is the parallel shift in GV from ions passing through the permeation pathway, and the other is the reduction of the slope of the GV curve caused by external thallium ions.

#### Shifting the GV Curve with Increasing Mole Fractions of Thallium

To establish how the concentration of permeating thallium affected the shift in the GV curve, currents were recorded from patches with external potassium and internal solutions with varying concentrations of thallium relative to potassium.

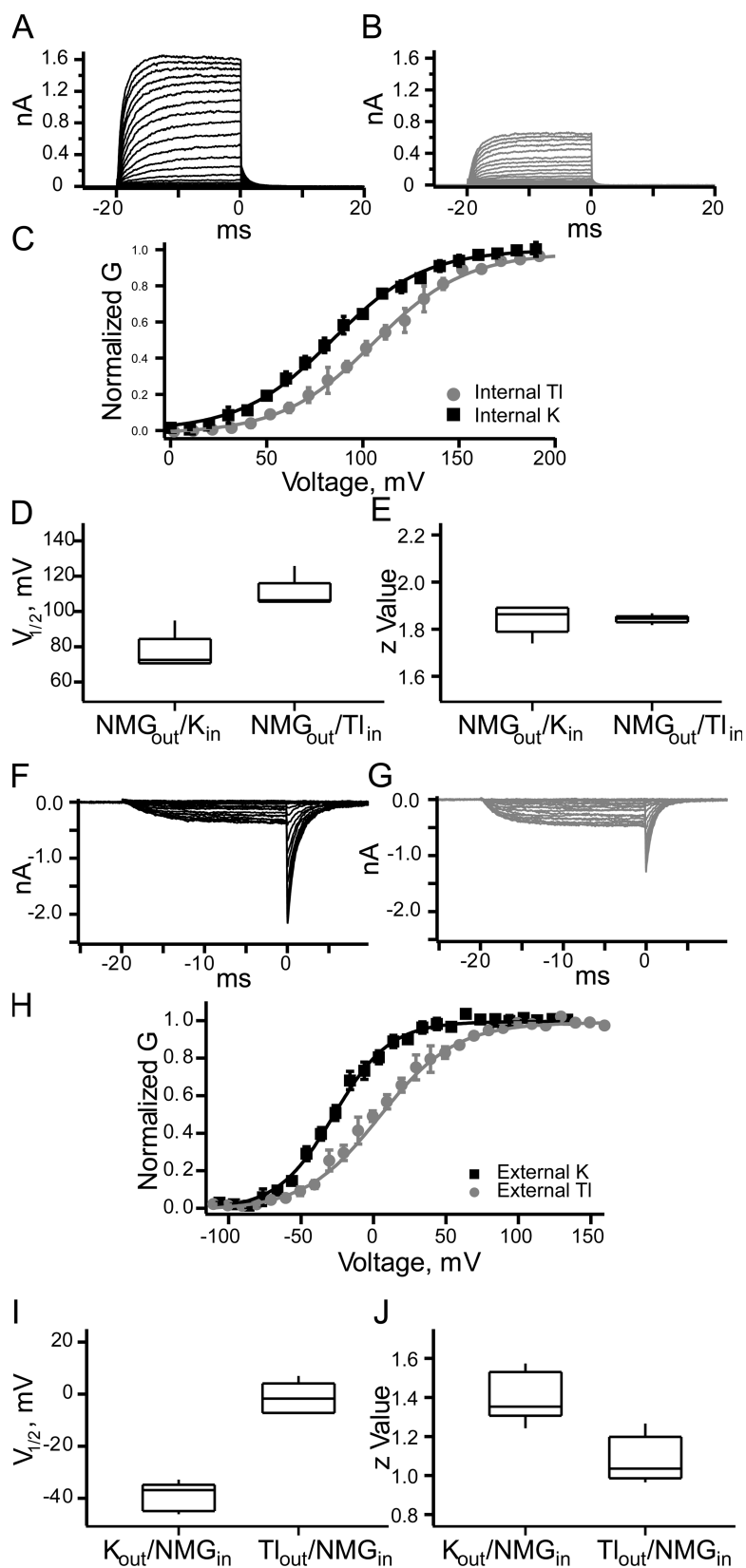
The  $V_{1/2}$  was shifted to higher potentials as the fraction of thallium in the internal solution was increased. These experiments were done with 2  $\mu\text{M}$  internal calcium. The channels would primarily be open at more positive potentials and the currents outward. The  $V_{1/2}$  from these experiments are plotted in Fig. 5 A. The  $V_{1/2}$  stopped increasing at 40–50 mM internal thallium and remained constant as the fraction of thallium was increased further.

Fig. 5 B shows the single channel current amplitude at 70 mV for several patches recorded under the same conditions as the data shown in Fig. 5 A. Potassium is able to permeate better than thallium, so when potassium is the only internal permeant ion, outward currents are  $\sim 13$  pA. As the potassium is replaced by thallium, the single channel current decreases as internal thallium is increased. At  $\sim 40$  mM, the single channel current magnitude does not change as potassium is replaced by thallium. The thallium concentration dependence is similar for the GV curve shift and the single channel current, further supporting the idea that the effect of thallium on gating occurs as a result of pore occupancy.

#### Application of Scheme I: Thallium Does Not Alter the Calcium Activation Pathway

To determine how permeating thallium is altering the gating of the BK channel, the model shown in Scheme 1 was applied. Fig. 6 A shows the currents recorded from two patches recorded with three different internal calcium concentrations and either symmetrical potassium or symmetrical thallium.

In the absence of calcium (10 mM internal EGTA), thallium altered the GV curve much as it does at higher calcium concentrations. There was an  $\sim 32$ -mV shift to higher potentials in the  $V_{1/2}$  of the GV curve. To alter the activity of the channel in the absence of calcium, thallium would have to be altering a gating process that does not require calcium binding such as voltage sensor



**Figure 4.** Gating effect from internal permeant ions. (A) Currents from an inside-out patch with external NMG and internal potassium. (B) Currents from an inside-out patch with external NMG and internal thallium. (C) The GV curves from multiple experiments. (D) Box plots of the  $V_{1/2}$  from Boltzmann fits of all the data with external NMG. (E) Box plots of the z values from Boltzmann fits ( $n = 6$  for potassium and  $n = 5$  for thallium). (F) Currents from an inside-out patch with internal NMG and external potassium. (G) Currents from an inside-out patch with internal NMG and external thallium. (H) The GV from multiple experiments. (I) Box plots of the  $V_{1/2}$  from Boltzmann fits of all the data with external NMG. (J) Box plots of the z values from Boltzmann fits. ( $n = 11$  for potassium and  $n = 13$  for thallium).

activation or channel opening. However, even though these results in the absence of internal calcium show that thallium alters a gating mechanism different from

calcium dependence, they do not rule out the possibility of additional effects of thallium on the calcium activation mechanism.

To understand further how thallium alters BK channel gating, the GV were measured for both symmetrical thallium and symmetrical potassium at seven calcium concentrations: 0, 2, 5, 10, 50, 100, and 300  $\mu\text{M}$ . For all seven calcium concentrations, currents recorded in symmetrical thallium had approximately the same shift in the GV curves compared with currents recorded in symmetrical potassium. The  $V_{1/2}$  values are plotted as a function of calcium concentration for both symmetrical potassium and symmetrical thallium solutions in Fig. 6 C. The difference in  $V_{1/2}$  as a function of calcium is shown in Fig. 6 D. These results show clearly that the thallium-induced shift in activation to more positive voltages is independent of calcium concentration.

Fig. 6 E shows that the external thallium-induced change in GV curve slope is also independent of calcium concentration. With symmetrical potassium solutions, the slope of the GV curve is around  $1.6 \pm 0.2$  in the absence of internal calcium. GV curves from currents recorded with symmetrical thallium solutions consistently decreased the slope by 20%, to  $1.3 \pm 0.14$ .

#### Application of the Coupled Allosteric Model

The coupled allosteric model (Scheme 1) was used to fit the GV curves from currents recorded with potassium or thallium solutions. To simplify the analysis, the

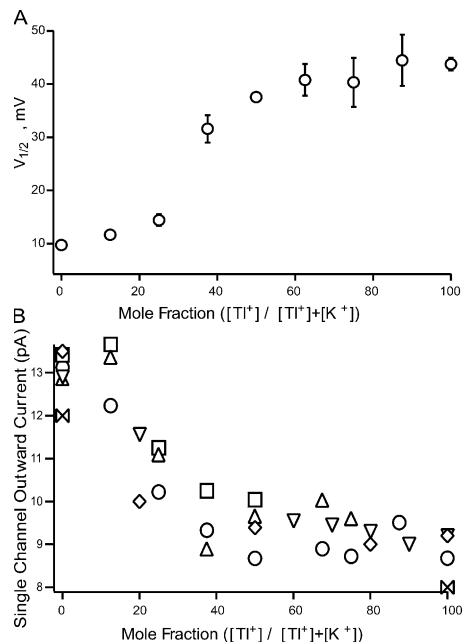


**Figure 5.** The shift in the GV curve as internal potassium is replaced by thallium. (A)  $V_{1/2}$  from Boltzmann curve fits plotted as a function of the concentration of internal thallium. (B) The single channel current at 70 mV as a function of the concentration of internal thallium. The different symbols represent data recorded from different patches. All patches were recorded in external potassium and 50  $\mu\text{M}$  internal calcium. The osmolarity is balanced by potassium.

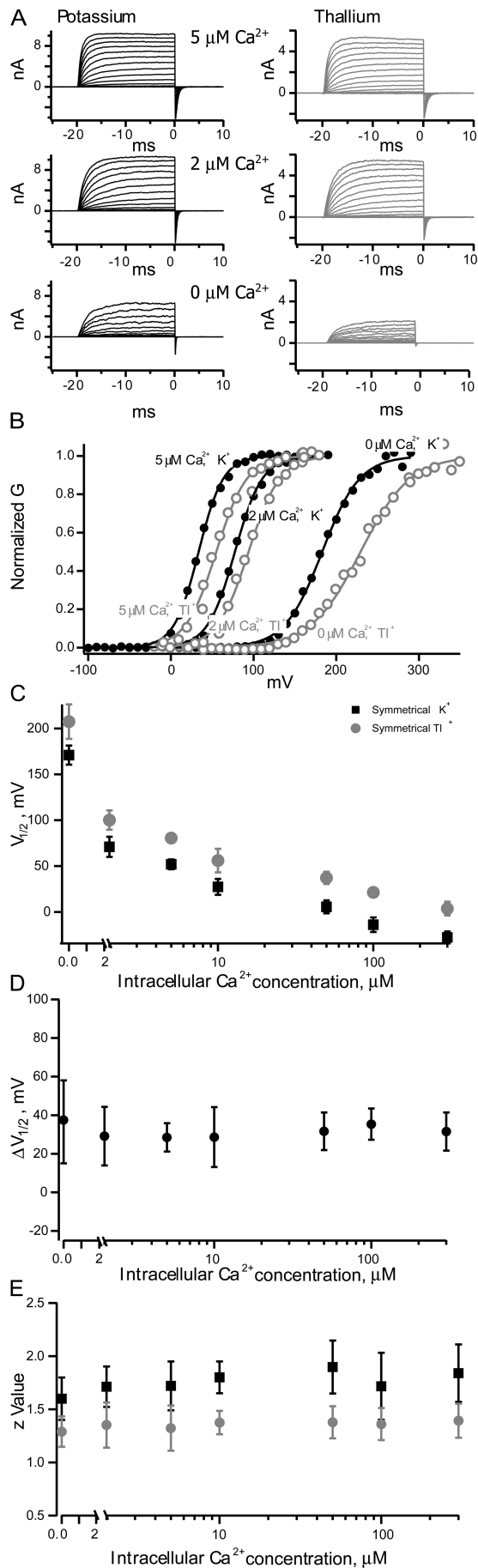
shift in the GV curves caused by permeating thallium was examined independently of the external effect of thallium. This was done by limiting the data to experiments with external potassium and either internal potassium or thallium. Curves from data recorded with different calcium concentrations were fit simultaneously (Fig. 7). For curve fitting, one or two parameters were allowed to vary while the others were constrained. The results of these fits are in Table II.

Simultaneous fits of GV curves with the coupled allosteric model revealed that the vast majority of the effect of permeating thallium could be accounted for by increasing  $L$ , the closed to open transition equilibrium constant. The fits of the data were not improved if any of the other parameters were allowed to vary. This result indicates that permeating thallium is disrupting the equilibrium between the open and closed states of the channel while not altering the voltage or calcium activation pathways.

The external effect of thallium was also examined by fitting GV curves with the coupled allosteric model (Scheme 1). GV curves from data recorded with either external thallium or external potassium and various calcium concentrations with internal potassium were fit simultaneously. The external effect of thallium could be accounted for in two ways. First of all, reasonable fits to the data were achieved by changing both  $L$ , the equilibrium constant between the open and closed states, and by reversing the sign of  $Q$ , the voltage dependence assigned to  $L$ . A change in the sign of  $Q$  would indicate that charges may move in the opposite direction across the electric field upon channel opening in the presence of external thallium. However, this change in sign would predict the deactivation time constants to increase at very negative voltages, which is inconsistent with our data (Fig. 2). If the value of  $Q$  was constrained and  $L$  alone allowed to vary, the fits were slightly off at the base of the GV curves.

However, the external effect of thallium could also be reproduced with the model by changing  $L$  along with  $D$ , the allosteric factor describing interactions between voltage sensor activation and channel opening, as well as  $V_{\text{hc}}$ , the half activation voltage of the closed state of the channel. As shown in Table I,  $D$  is the factor by which opening of the channel is enhanced by voltage sensor activation, and  $V_{\text{hc}}$  is the voltage at which the voltage sensors are half activated in the closed state. Changes with these parameters would indicate that external permeant ions are altering the response of the voltage sensors (i.e.,  $J$ ) and/or altering the ability of the voltage sensors to promote opening (i.e.,  $D$ ). Unfortunately, it is impossible to differentiate the effects of external thallium on voltage sensor activation and allosteric activation with this data. Hence, the exact mechanism of the external effect of thallium on voltage activation remains elusive.





### Fitting Data at Very Low Opening Probability

For the coupled allosteric model to account for the permeating effect of thallium, a change in  $L$  alone was sufficient. Fitting the GV curve with the model was a useful way to isolate parameters that have been potentially altered in the gating process. To further test the hypothesis that the open-closed equilibrium ( $L$ ) is primarily being altered when thallium is permeating the channel, data collected at very low open probabilities were fit with the model. At these very low voltages it is possible to isolate opening and closing transitions without activation of voltage sensors (Horrigan and Aldrich, 2002).

The voltage dependence of the opening probability at very low voltages is an estimate of  $Q$ . If there is a change in the concerted opening voltage dependence, then the slope of the low open probability plot would be expected to change. The open probability ( $NP_O$ ) was measured with inside-out patches that contained hundreds to thousands of channels, and was estimated in two separate ways:  $NP_O$  was determined from all-points amplitude histograms by measuring the fraction of time spent ( $P_K$ ) at each open level ( $k$ ) using a half-amplitude criteria and summing their contributions  $NP_O = \sum k P_K$ .  $NP_O$  was also determined by fitting  $P_K$  with a Poisson distribution  $P_K = e^{-NP_O} (NP_O)^k / k!$ . Both of these methods resulted in  $NP_O$  values that agreed within 3% consistent with the assumption that the observed currents represent the activity of a large uniform population of channels opening with very low probability (Horrigan et al., 1999; Horrigan and Aldrich, 2002). Plots of  $NP_O$  are shown for several different patches in Fig. 8 (A and B).

The slopes of the  $NP_O$  voltage curves did not significantly differ for currents recorded with symmetrical potassium ( $0.35 \pm 0.116$ ,  $n = 11$ ) or with external thallium and internal potassium ( $0.36 \pm 0.15$ ,  $n = 12$ ). This lack of change in slope indicates that the voltage dependence of the concerted opening transition is not altered by external or permeating thallium. Therefore external thallium is probably altering the voltage activation of the channel by acting through the voltage sensor activation pathway.

To test the results more completely, plots of the  $\log P_O V$  curve were fit with the coupled allosteric model. For these experiments, the opening probability was measured

**Figure 6.** Calcium activation of BK channels in symmetrical potassium and thallium solutions. (A) Two patches with either symmetrical potassium (black) or symmetrical thallium (gray) at three different calcium concentrations. (B) Averages of GV curves from multiple voltage families from the patch shown in A. (C) Plot of  $V_{1/2}$  from Boltzmann fits at multiple calcium concentrations for symmetrical potassium solutions (black squares) and symmetrical thallium solutions (gray circles). (D) The difference in the  $V_{1/2}$  at each calcium concentration for symmetrical thallium and potassium. (E) The  $z$  values from Boltzmann fits of GV curves from patches with external potassium (black squares) or external thallium (gray circles).

TABLE II  
Steady-state Parameters

	$L_0$	$Q$	$z$	$V_{hC}$	$K_D$	$C$	$D$	$E$
Parameters that describe symmetrical potassium	$1.67 \times 10^{-6}$	$0.3 e$	$0.58 e$	150 mV	11 $\mu$ M	8	30	2.4
Parameters that can account for external thallium, $L$ and $Q$	$9.7 \times 10^{-7}$	$-0.3 e$	$0.58 e$	150 mV	11 $\mu$ M	8	30	2.4
Parameters that can account for external thallium, $L$ , $D$ , and $V_{hC}$	$4 \times 10^{-8}$	$0.3 e$	$0.58 e$	84 mV	11 $\mu$ M	8	15	2.4
Parameters that can account for permeating thallium	$2.3 \times 10^{-5}$	$0.3 e$	$0.58 e$	150 mV	11 $\mu$ M	8	30	2.4

over a very wide range of voltages ( $-160$  to  $300$  mV). This wide range of voltages presented a problem: external thallium alters the voltage activation of the channel and measurements of the opening probability at negative voltages with permeating thallium require external thallium. However, the  $NP_{OV}$  plots indicated that there was no significant difference in the voltage dependence of the opening probability with internal and external thallium at these voltages (Fig. 8, A and B, from ANOVA, with mean slopes of  $0.35$  and standard deviation of  $0.02$  for potassium and mean of  $0.37$  and standard deviation of  $0.06$  for thallium,  $P = 0.89$ ). The permeating effect of thallium could be isolated from the external effect by using data from patches with internal potassium and external thallium for negative voltages and data from patches with external potassium and internal thallium

for positive voltages. In this way,  $P_O$  was estimated from the  $NP_O$  when the number of channels could be approximated. Fig. 8 C shows a plot of the  $\log P_O$  for permeating thallium and symmetrical potassium. The points presented in Fig. 8 C are data from one experiment in which currents were recorded at a very wide range of voltages. The solid lines are from fits with the coupled allosteric model with values from simultaneously fitting data from multiple experiments. The permeating thallium data were fit with all of the same parameters as the potassium data with only  $L$  being the free parameter. Allowing the other free parameters to vary independently along with  $L$  did not improve the overall fit.

#### Thallium Increases the Flicker of the BK Single Channels

As reported previously for BK channels (Blatz and Magleby, 1984), the single channel conductance of thallium is  $\sim 20\%$  less than that of potassium. The currents shown in Fig. 9 (A and B) were recorded with external NMG in the pipette. The two traces are from the same patch with either internal potassium or internal thallium. These currents were recorded with  $10$  mM internal EGTA and no added calcium.

As can be observed from the single channel records in Fig. 9, thallium increases the number of short flicker closings. These short closing events have been previously characterized (Blatz and Magleby, 1984; Rothberg and Magleby, 1998; Talukder and Aldrich, 2000). The open and closed durations are plotted in dwell time histograms (Fig. 9, C and D). There is a larger proportion of longer open dwell times for the potassium data than for the thallium data. The average time that the channel spent in the open conductance level before closing was  $\sim 1.1$  ms with potassium as the internal ion, whereas with thallium as the permeant ion, the average time that the channel spent at the open conductance level before closing was around  $250 \mu$ s. Channels conducting thallium stay open for briefer times than channels conducting potassium.

The closed duration histograms also reveal differences in gating induced by thallium. As mentioned earlier, the  $P_O$  for the channel with internal potassium was higher than the  $P_O$  with internal thallium. The histograms for both the internal potassium and internal thallium data have two easily distinguished populations of

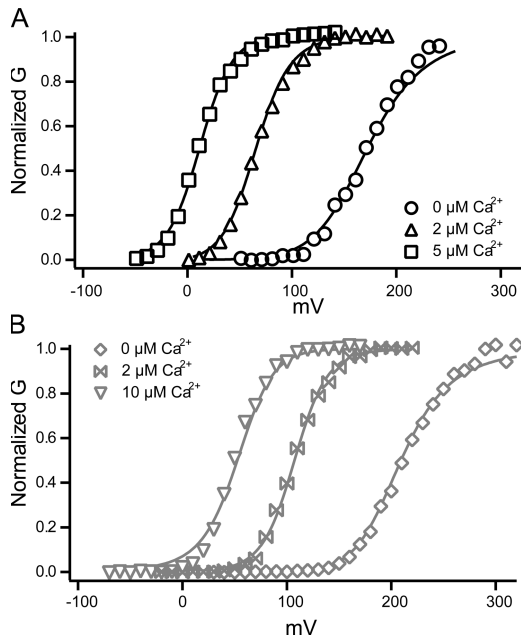


**Figure 7.** Simultaneous fits of GV curves with the allosteric model of Scheme 1. The top graph has data from three different calcium concentrations in symmetrical potassium solutions. The solid lines are fits with the 70-state model. All the calcium concentrations were simultaneously fit. The lower graph has data from the same patch in the top panel, except with internal thallium and three concentrations of calcium. The solid curves are fit with the Scheme 1.

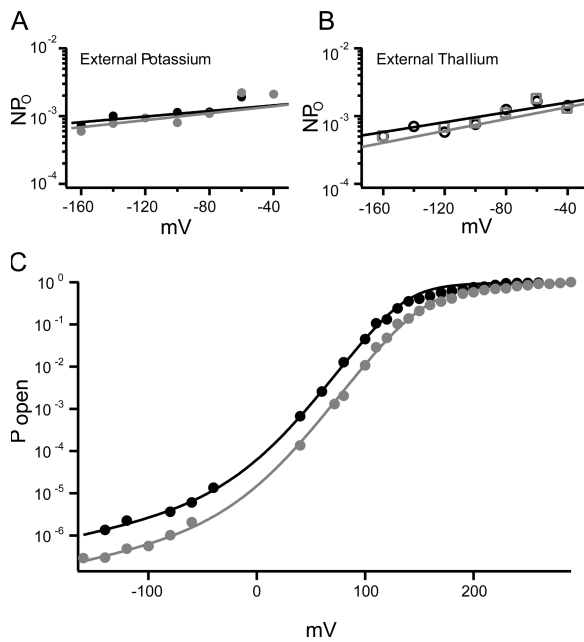


**Figure 8.**  $NP_O$  for external potassium and external thallium.  $NP_O$  versus voltage plots from these two patches are being used as an example because their  $N_s$  are in the same range. (A)  $NP_O$  at very low voltages for external potassium with internal potassium (solid black circles) or internal thallium (solid gray circles). (B)  $NP_O$  at very low voltages for a patch with external thallium and with internal potassium (open black circles) or internal thallium (open gray squares). (C) Fit of  $\log P_{open}$  with the seventy state allosteric model. The opening probability over a very wide range of voltages for symmetrical potassium (black circles) and from  $-160$  to  $0$  mV external thallium with internal potassium and from  $0$  to  $+300$  mV internal thallium with external potassium (gray circles).

closed times; one with a mean closed duration of  $\sim 8$  ms and another with a mean of  $\sim 100$   $\mu$ s. The  $P_O$  measured from these traces is  $\sim 0.4$  with internal potassium and  $\sim 0.2$  for internal thallium. When thallium is the conducting ion, the short flicker closed events far outnumber the longer closed events. The increased number of short flicker events is primarily responsible for the decreased  $P_O$  for thallium currents.

How is flicker dependent on the concentration of thallium? To answer this question, single channel currents were recorded at  $70$  mV with external potassium and a varying mole fraction of thallium and potassium in the internal solution. Fig. 10 A shows how the mean open time decreased as the fraction of thallium was increased.

A useful metric for assessing the prevalence of the flicker closed states is examining the number of openings separated by brief flicker closed events. The sets of openings, or bursts, are separated by longer-lived closed events. For this analysis, bursts were defined as series of openings that were separated by closing events  $>1$  ms. To determine how sensitive the data were to the burst criteria, the data were analyzed with closed-time cutoffs with  $500$   $\mu$ s,  $750$   $\mu$ s, and  $1.1$  ms; the results were found not to

significantly differ in this range of burst criteria. As internal thallium replaced internal potassium, the number of openings per burst increased until the internal thallium was  $\sim 50$  mM and then remained constant (Fig. 10 B). The mean open duration also followed a similar pattern, decreasing until the internal solution was  $\sim 50$  mM and then not changing as the fraction of thallium was increased. Both the decrease in open time and the increase in flicker are dependent on the concentration of thallium and correlate with the mole fraction effects seen with the GV shift induced by internal thallium, and single channel current amplitudes (Fig. 5, A and B). For all four phenomena, the channel gating behavior is altered as potassium is replaced by thallium over similar concentrations: the single channel current decreases, the GV shifts to higher potentials, the number of flicker-closed events increases, and the mean open time decreases.

An additional experiment was performed to further test the theory that thallium is inducing this increase in flicker by acting through the permeation pathway. In these experiments, single channel currents were recorded with external potassium in the pipette. The concentration of internal permeant ion (either potassium or thallium) was decreased while the osmolarity of the internal solution was adjusted with different concentrations of impermeant species NMG or sucrose. It is assumed in this case that the selectivity filter will be occupied by external permeant ions at positive potentials when the internal solution lacks permeant ions. As permeant ions are added to the internal solution, it is expected that the selectivity filter will gradually be occupied by ions from the internal solution. As permeant ions are readily available on both sides of the membrane, the selectivity filter will be primarily occupied by the internal ion at positive potentials.

The results of these experiments are shown in Fig. 11. The currents recorded with increasing potassium solutions show a fairly constant mean open duration at potassium concentrations  $>40$  mM. The mean open durations with internal potassium at concentrations  $<40$  mM are slightly reduced. This reduction in mean open duration is most likely due to contamination by false threshold crossing by noise as the single channel current decreased. The noise was approximately on the order of  $0.2$ – $0.5$  pA and the smallest single channel current was on the order of  $1$ – $2$  pA for potassium solutions and  $0.7$ – $1.2$  pA for thallium solutions. As a result of this, the potassium data is skewed a bit to lower mean open times at lower potassium concentrations. This same influence of noise is probably also corrupting the data from internal thallium concentrations. However, as thallium is increased, the mean open duration decreases. For currents recorded with internal thallium, the number of openings per burst increased as the concentration of thallium increased until thallium was  $\sim 40$  mM and then saturated. The number of openings per burst did

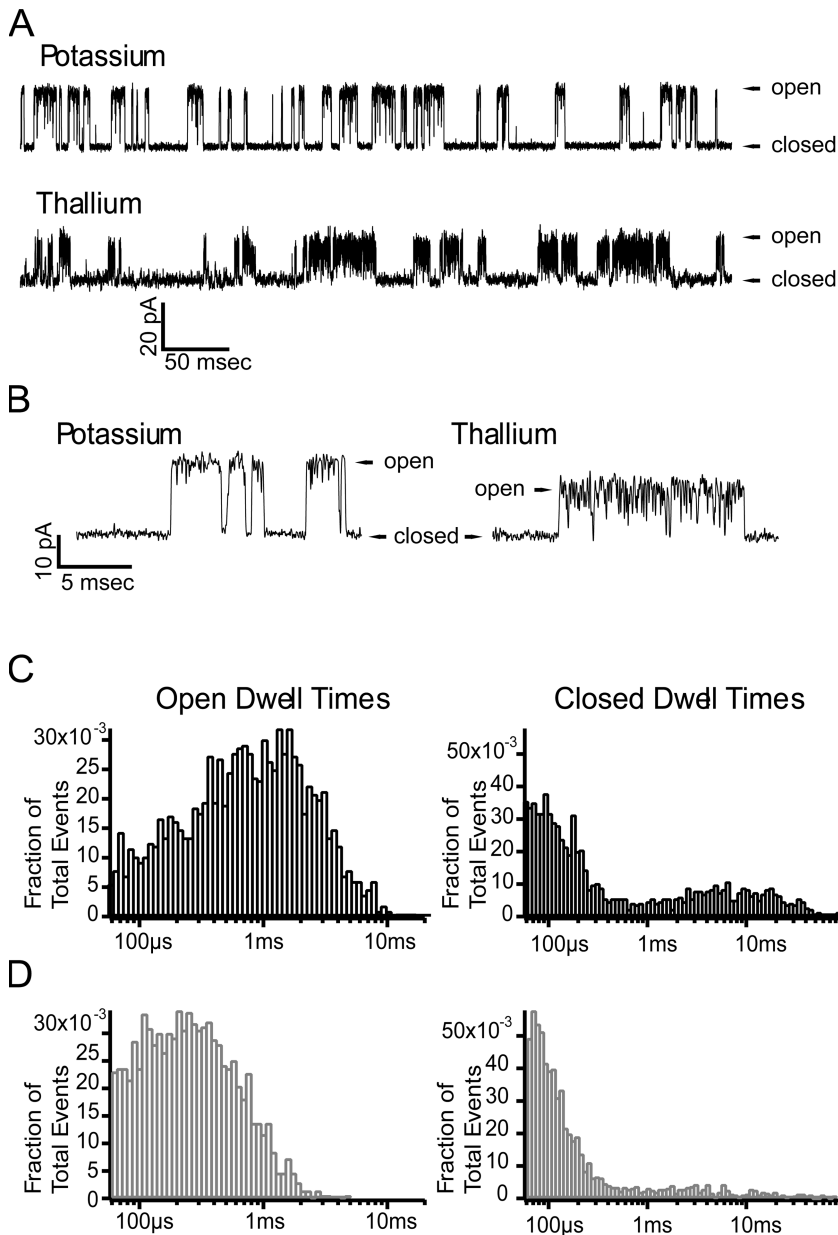


**Figure 9.** Single channels currents from the same inside-out patch. (A and B) The external solution (pipette) contained 100 mM NMG and the internal solution (bath) contained either 100 mM potassium or 105 mM thallium. This data was recorded at +150 mV with 0  $\mu$ M internal calcium. (C and D) Open and closed dwell time histograms from the same patch shown in A and B. Black bins are from currents measured with internal potassium and gray bins are from currents measured with internal thallium.

not show any dependence on the concentration of internal potassium.

#### Flicker at Low Opening Probability

To investigate how permeant thallium is affecting the concerted opening transition of BK channels, the single channel behavior was investigated under conditions where the probability of a single channel opening event would be very low. Recordings were made in the presence of internal EGTA at negative voltages (-160 to -40 mV). Under these conditions, calcium is not present to activate the channel, so the coupled allosteric model can be simplified to a 10-state MWC model with voltage sensor activation in subunits activating the channel. At very low voltages, there is an extremely low probability that any voltage sensors would be activating.

Under these conditions, a single channel has an open probability  $<10^{-6}$ . Currents were recorded from traces with hundreds to thousands of channels in the patch. Because of the very low opening probability for each channel, under these conditions two opening events occurring at the same time was extremely rare.

According to the model, there are only a very small number of states being visited under these conditions. Normally, methods of fitting duration histograms could yield information about the kinetic rates between the states and be used to refine the kinetic model. This method of analysis has not been done here for two reasons: the limited resolution of very short events and the large number of channels in each patch.

Even though the lifetimes of many events are not resolved due to bandwidth limitations, longer events are

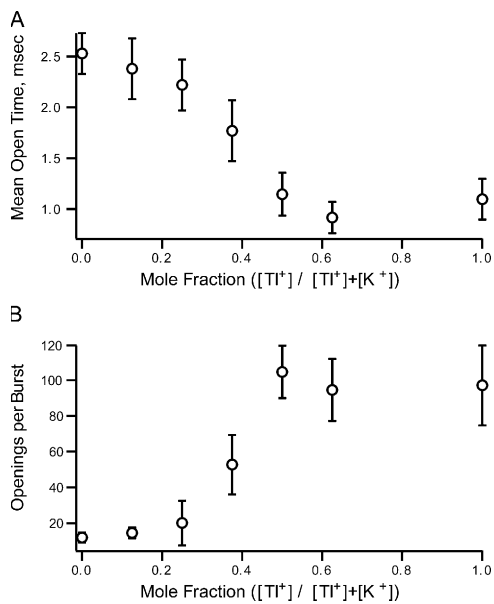


**Figure 10.** Mole fraction effects on the mean open time and number of openings per burst. At point 0 on the x axis, the internal solution was 100 mM potassium. The potassium in the internal solution was replaced by thallium until the internal thallium concentration was 100 mM. Potassium solutions were external for all experiments and the membrane potential was held at 70 mV. (A) The mean open time decreased as thallium replaced potassium. (B) The number of openings per burst increased as the fraction of thallium increased.

still detected. It is reasonable to assume that comparison of detected open dwell times between potassium and thallium would still yield information about how thallium alters gating at low opening probability. Fig. 12 A plots the average measured open duration for currents recorded with either external thallium or potassium and internal potassium. The measured open time for potassium is  $\sim 20\%$  longer than the average open time for thallium.

For these data, the number of very short flicker closings observed during opening events was analyzed (Fig. 12 B). This analysis is based on the assumption that the flicker closing events seen during an opening event from one channel are due to gating events from that same channel. Under these conditions there were no observed instances where more than one channel opens at the same time. With potassium as the permeant ion, flicker closings were observed in  $4 \pm 1\%$  ( $n = 11$ ) of the events. With thallium as the permeant ion,  $\sim 15 \pm 2\%$  ( $n = 10$ ) of the openings contained at least one short flicker closing. These differences are statistically significant with a P value  $< 0.0001$ . This detection of short-lived flicker states indicates that there is more than one closed state that the channel can occupy under these conditions. While potassium is the permeating ion, a larger proportion of longer open times is detected than when thallium is the permeating ion. Also, even though

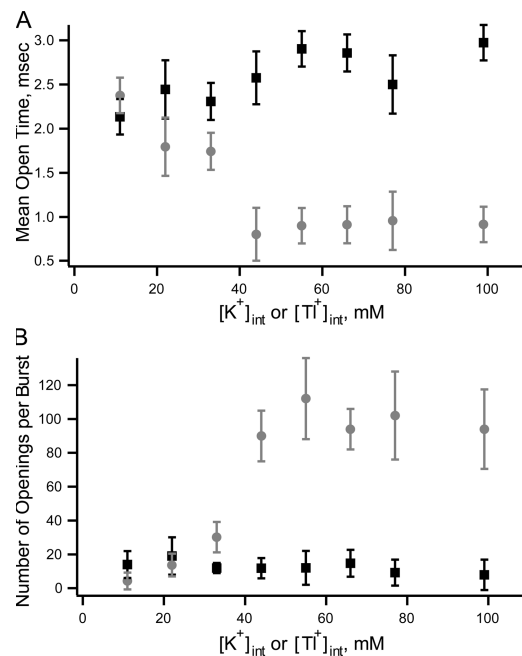


**Figure 11.** Concentration dependence of the mean open time and number of openings per burst. Increasing concentrations of potassium (black squares) had little to no effect on the mean open time and number of openings per burst. However, increasing concentrations of thallium (gray circles) decreased the mean open time and increases the number of openings per burst. Membrane potential was held at 70 mV.

there is a decrease in the number of longer-lived opening events with thallium, there is an increase in the number of short flicker closings. The detected open times may be longer with potassium for two reasons: the open state may be more stable or the lifetimes of the flicker events may be too short to be detected, causing the openings to appear unnaturally longer. To qualitatively address these questions, lifetimes of the brief closed events were tallied for both conditions. The average detected closed flicker time did not significantly differ between permeant potassium ( $92 \pm 13 \mu s$ ,  $n = 11$ ) and permeant thallium ( $89 \pm 11 \mu s$ ,  $n = 10$ ), by ANOVA,  $P = 0.9992$ . Because of the large number of undetected events, these results are not conclusive. However, this does provide evidence that the flicker closings exist at very low opening probability and do not require calcium binding or voltage sensor activation. It is possible that much of the 20% difference in mean open times between thallium and potassium conditions is a result of the increased occurrence of flicker closings. The actual flicker closed state is itself not altered by thallium, only the chance of entering it from the open state.

**Increase of Flicker by Thallium at High Opening Probability**  
To test further whether thallium is altering the stability of the flicker state, data was collected at higher opening probability. At 300  $\mu M$  internal calcium and voltages

>50 mV, the channel is maximally open while potassium or thallium is permeating.

At very high opening probabilities, the dwell time histogram for the closed conductance level is dominated by a large number of flicker closing events (Talukder and Aldrich, 2000). If permeating thallium is only altering the probability of the channel to enter the flicker state from the open state, and not actually altering the ability of the channel to leave the flicker state, then no change would be expected in the closed time histograms under these conditions. To test this hypothesis, currents were recorded in patches with external potassium solutions and either internal potassium or thallium. Fig. 13 shows the dwell time histograms for a patch recorded at +50 and +70 mV with either potassium or thallium in the internal solution. The open dwell-time histograms are shifted to shorter lifetimes when thallium is the permeating ion. For potassium, the average open dwell-time was between 2.5 and 3.0 ms. For thallium, the average open dwell-time was reduced to ~1.0–1.5 ms. There were no detectable differences in the closed dwell-time distributions for permeating thallium and permeating potassium for all seven of the patches examined.

These results support the theory that thallium is enhancing the probability that the channel will enter a short-lived flicker state once it is in an open state. The

stability of the flicker state itself is not apparently affected by permeating thallium because the closed lifetimes are not apparently different. Can the flicker state access the closed state? If the flicker state can only be accessed via the open state, then it would be predicted that the total open time per burst would be unchanged between potassium and thallium. The mean open time, the number of openings per burst and the mean total open time per burst were compared between currents with permeating potassium ( $n = 3-6$ ) and thallium ( $n = 4-6$ ) (Fig. 14).

The mean open time decreased with thallium permeation from +30 to +90 mV (Fig. 14 A). The number of openings per burst also increased, indicating an increase in the number of short flicker closings between openings (Fig. 14 B). The mean total open time per burst, the product of the mean open time and number of openings per burst, slightly decreased when thallium was the permeant ion (Fig. 14 C), suggesting a possible pathway between the flicker state and the long-lived closed state. However, such a pathway has not been conclusively proven in this experiment; the difference between the thallium and potassium data is not very substantial. Extensive single channel analyses have shown that BK single channel kinetics require multiple open and closed states to account for the data (Blatz and Magleby, 1984; Rothberg and Magleby, 1998; Talukder and Aldrich, 2000); thus, this complex kinetic behavior may mask the effect of thallium on the stability of the open state with this measurement.

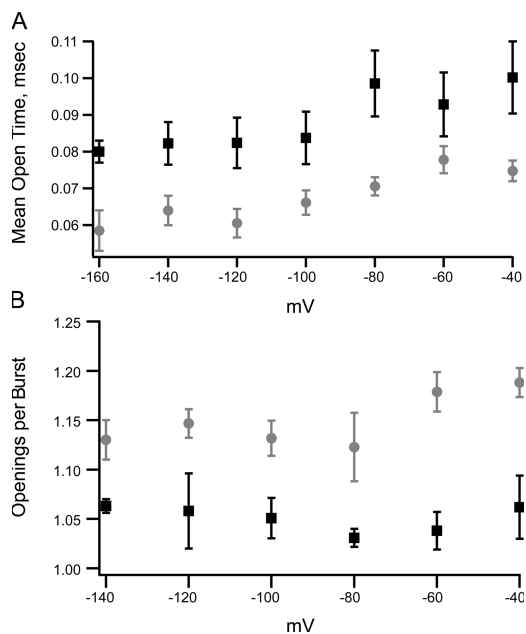


**Figure 12.** (A) Mean open time (overestimate) from patches containing multiple channels. Symbols are the average  $\pm$  SEM of mean open durations from patches with symmetrical potassium (black squares,  $n = 10$ ) or internal potassium and external thallium (gray circles,  $n = 9$ ). (B) Average number of openings per burst recorded at very low  $P_O$  for currents recorded with potassium (black squares,  $n = 10$ ) and symmetrical thallium (gray circles,  $n = 11$ ).

## DISCUSSION

Thallium affected gating of the BK channel in two ways: thallium on the external face of the channel alters the voltage sensitivity of the channel as evidenced by the decrease in the slope of the GV curve; and thallium as the permeating ion alters the opening and closing transition as evidenced by the parallel shift in the GV curve and also increases the number of single channel flicker events. Calcium activation of the channel was not altered in either condition.

### External Effect of Thallium

External thallium was found to decrease the slope of the GV curve. This external effect was independent of the permeating ion. This was analyzed by fitting GV,  $NP_O$  vs. voltage, and  $\log P_O$  vs. voltage plots with the coupled allosteric model. The parameters representing the equilibrium for voltage sensor activation in the closed channel ( $V_{hc}$ ) had to be adjusted to account for the changes in gating induced by thallium. Additionally, the allosteric factor that describes enhanced opening by voltage sensor activation (D) also had to be adjusted, as well as the equilibrium between the closed and open states (L). A mechanistic interpretation of

these modeling results would be that external thallium inhibits motion of the voltage sensor for the closed and the open channel and/or inhibits the voltage sensors from enhancing the opening of the channel. It was also possible to account for all of the external thallium effects by changing the closed–open equilibrium ( $L$ ) and its voltage dependence ( $Q$ ). The deactivation time constants did not increase at negative potentials, nor was there a change in the slope of  $NP_O$  at very low probabilities. Both of these results are incompatible with a change in  $Q$ . We therefore favor the former interpretation.

In BK channels, neutralization of the aspartic acid in the GYGD signature sequence had dramatic effects on the voltage gating of the channels. The activation curves of the channel were shifted by  $\sim 20$  mV to more depolarized potentials (Haug et al., 2004a). It was concluded from gating current measurements that the voltage sensors are not affected, but that the voltage sensitivity of the concerted allosteric opening transition is reduced. The authors state that the neutralization of this residue reduces the stability of the open state (Haug et al., 2004a). Perhaps external thallium is inducing a similar destabilizing effect on the external face of the selectivity filter.

External ions have been found to alter the voltage gating in *Shaker*,  $K_V1.5$ , and  $K_V2.1$  channels. For *Shaker*, external barium was found to increase the rate of off gating currents (Hurst et al., 1997). It was concluded that barium binding in the selectivity filter destabilized the open state and enhanced closing (Hurst et al., 1997). Similar results were seen with  $K_V1.5$ , where extracellular cesium and rubidium accelerated the off gating currents (Wang et al., 1999). For  $K_V2.1$ , the on gating currents were increased with the presence of permeating ions (Consiglio and Korn, 2004). For all of these cases, external ions alter the stability of the open state. External thallium may be acting through a similar mechanism.

Consiglio and Korn (Consiglio et al., 2003; Consiglio and Korn, 2004) proposed that the outer vestibule of the selectivity filter is only a few angstroms away from the voltage sensor. They stated that possible conformational changes in the selectivity filter could allosterically

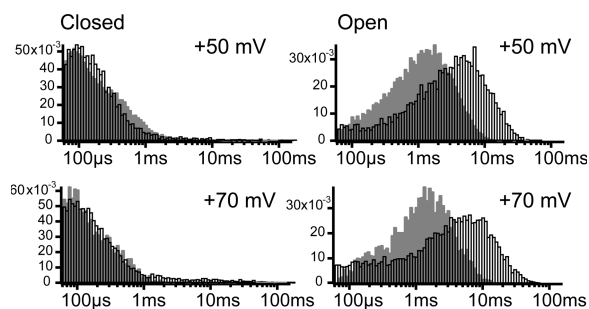


**Figure 13.** Duration histograms from one patch with either internal potassium (black bars) or internal thallium (gray bars) solutions. Potassium solutions were in the pipette.

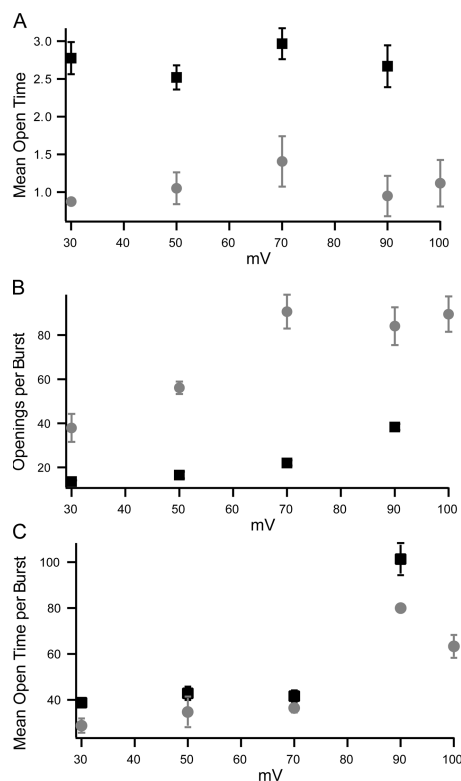


**Figure 14.** Results of further single channel analysis at high  $P_o$ . (A) The mean open duration for currents with potassium as the permeating ion (black squares) or thallium as the permeating ion (gray circles). (B) The mean number of openings per burst for the two conditions. (C) The mean open time per burst for the two conditions. This value is the product of the mean open time and the number of openings per burst for each patch.

translate to the S4 and impede activation or deactivation. This theory can also be applied to the effect of external thallium. Because thallium is much more electronegative than potassium, it is possible for it to form stronger interactions with backbone carbonyl oxygens, or side chains in the outer vestibule of the selectivity filter. These interactions may be altering the structure, and hence altering the voltage activation of the channel. Such a close interaction between the voltage sensors and the external vestibule, however, would be incompatible with the published structure of  $K_V1.2$  (Long et al., 2005a, 2005b); however, it is conceivable that they are closer in different gating states.

#### Permeating Effect of Thallium

Permeating thallium caused a parallel shift in the GV curve for macroscopic currents. The time course of deactivation was also decreased. At the single channel level, permeating thallium increased the number of short flicker events. Qualitatively, all of these results indicate that the open state of the channel is destabilized by thallium. The coupled allosteric model could account for the change in kinetics if the parameter

representing the equilibrium between the closed and open states,  $L$ , was adjusted. Single channel analysis revealed that permeating thallium decreased the mean open time and increased the presence of flicker closings at very low and at very high opening probability. This change in the single channel kinetics can also be accounted for by altering  $L$ . Substantial changes in the other model parameters were not compatible with all of the experimental effects of permeating thallium on channel gating. We are confident that permeating thallium alters the gating behavior of BK channels by altering the allosteric opening and closing of the channel ( $L$ ), and minimally affects the other gating properties of the channel such as calcium and voltage activation.

#### Relating Changes in Flicker to the Macroscopic Results

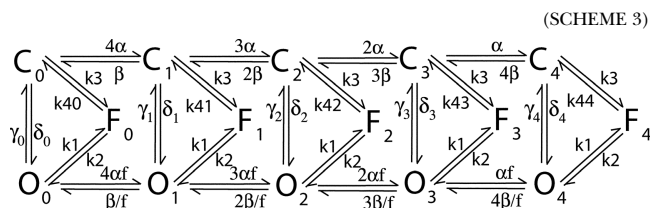
We have found that permeating thallium increases the incidence of flicker at very low and at very high open probabilities. When the channels are maximally activated, the vast majority of closing events with permeating thallium are to the flicker state. Just as the GV curves were shifted by increasing mole fractions of thallium, the mean open time and flicker incidence also showed dependence on the mole fraction of thallium. The mean open time decreased and the number of openings per burst increased with increasing thallium. Additionally, the overall concentration of permeating thallium tended to shift the GV (i.e., alter  $L$ ) as well as increase the flicker at the single channel level. The similar concentration and mole fraction ranges for the GV shift and the flicker suggest that they may be due to the same processes.

#### Accommodation of Flicker into the Coupled Allosteric Model

An additional closed state separate from the activation pathway is required to adequately describe the flicker state (Rothberg and Magleby, 2000). To account for the flicker as well as the shift in the GV curve, we have added a single additional state,  $F$ , to the opening transition in Scheme 1, representing the short closed flicker events. Thallium increased the number of flicker events without altering the average lifetime of the detected closed state dwell times. This can be accounted for if thallium increases the transition rate from the open to the flicker state. Scheme 2 would be capable of accounting for the flicker at low and high open probabilities as well as the slowed deactivation rate in the presence of thallium.

Scheme 2 provides an alternative pathway for the channel to get from the closed to open conformation. If thallium increases the open to flicker transition (as required by the decrease in open duration), and if the channel can close from the flicker state (as suggested by the data in Fig. 14), then permeating thallium is decreasing the stability of the closed state relative to the open state. To test this hypothesis, Scheme 3, an

expanded form of Scheme 2, was used to simulate macroscopic currents. For these simulations, the calcium concentration was held at zero. Rate constants were constrained so that the voltage activation,  $D$ , would enhance the transition from closed to open by the same factor regardless of pathway. Fig. 15 shows a GV curve from simulated currents as well as the decrease in activation and deactivation rates. Table III lists the values of the parameters used for the simulation.



Scheme 2 can account for the behavior of these channels at very high and low opening probability. In this scheme, a nonconducting flicker state is accessible from both the closed and open states. The increase in flicker decreases the time the channel spends in the open state, and the connectivity of the model allows the channel to close from the flicker state, thereby reducing the overall opening probability even more. In this way, the activation curve of potassium channels is shifted to higher potentials.

#### A Proposed Molecular Mechanism for the Open State Destabilization by Permeating Thallium

We propose that the flicker state seen in the single channel data corresponds to the low- $K^+$  (collapsed) form of the selectivity filter seen in KcsA (Zhou et al., 2001; Zhou and MacKinnon, 2003; Lenaus et al., 2005). This is attractive for several reasons, based on parallels between our results on BK channels and studies of the thallium effects on structure and gating of KcsA. First of all, the equilibrium between the high  $K^+$  (conducting) structure and the collapsed structure of KcsA was affected by the permeant ion. In potassium and thallium solutions, the KcsA structure had two distinct and well-resolved structures at low and high concentrations of ions. There was a particular concentration for both potassium and thallium that the channel spent equal amounts of time in both structures, thus making the structure poorly resolved. For potassium solutions, this transition occurred at  $\sim 20$  mM; for thallium solutions the transition occurred at  $\sim 80$  mM (Zhou and MacKinnon, 2003). Higher concentrations of thallium than potassium ions were required to stabilize the conducting form of the selectivity filter. In other words, at a given concentration of ion, the equilibrium between the two structures is shifted toward the collapsed state by thallium. It is important to emphasize that the selectivity filter was seen to only have two well-defined states (Zhou and MacKinnon, 2003). There is no evidence that the



selectivity filter is wobbly, or has stable intermediates of the two states, compatible with a transition between two conducting states, open and flicker.

Second, as in BK channels, permeating thallium alters the single channel gating of KcsA. The openings are shorter, and there is an increase in the number of flicker closings in each opening burst (LeMasurier et al., 2001). This change in single channel kinetics would be predicted from structural information. If thallium increases the stability of the collapsed form of the selectivity filter in the crystallized state, then it can also stabilize the collapsed form when the channel is in a lipid bilayer. With thallium, KcsA only has one open channel conductance level (LeMasurier et al., 2001). This would be expected for the sharp conformational change occurring between the conducting and collapsed states of the selectivity filter. If the selectivity filter had a myriad of conformations, then there would be a continuum of open channel conductances. However, just as expected from the crystal structure, there is only one conductance level.

Finally, as in BK channels, the occurrence of the flicker in the single KcsA channel data shows dependence on the concentration of thallium. In mole fraction experiments, the single channel behavior changed as the potassium was replaced by thallium. In experiments with only thallium in the internal solution and potassium in the external solution, the single channel behavior changed as thallium was increased. For both of these experiments, the single channel kinetics stopped changing at around 40–50 mM of thallium, approximately the same concentration we have observed for BK channels. The shift in the GV by internal thallium also follows a similar behavior. This concentration may be right where the concentration of thallium is just enough to destabilize the conducting high- $K^+$  form.

The flicker observed with thallium solutions is present with potassium solutions and has been described and characterized multiple times (Barrett et al., 1982; Magleby and Pallotta, 1983; Blatz and Magleby, 1984; McManus and Magleby, 1988, 1991; Cox et al., 1997; Cui et al., 1997; Rothberg and Magleby, 1998, 1999; Nimigean and Magleby, 2000; Talukder and Aldrich, 2000). To account for the flicker in single channel data, extra closed states out of the activation pathway are necessary (Wu et al., 1995; Rothberg and Magleby, 1998, 1999). How much of a role does this potential selectivity filter conformational change play in the gating of the channel? As suggested by the two KcsA structures, the conformational change at the selectivity filter would not alter the structure of the channel outside of the selectivity filter. This also seems to apply to the two possible structures of the BK selectivity filter. Increasing the flicker with thallium had no effect on the calcium activation or the voltage activation of the channel. The decrease in the open duration can be accounted for by adding a flicker state, and not altering the opening or

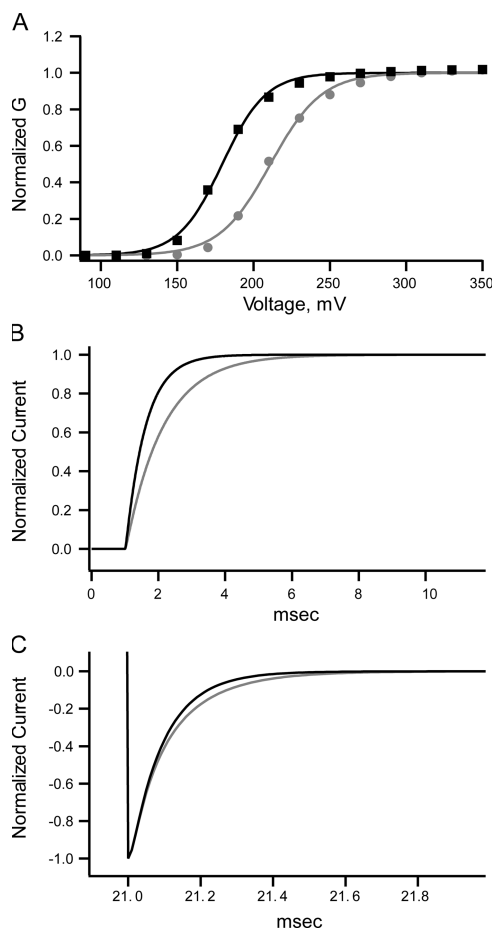


**Figure 15.** Simulated data with Scheme 3. (A) GV curves calculated from currents simulated with Scheme 3 with parameters that can account for permeating potassium (black trace) and permeating thallium (gray trace). The kinetic effects of permeating thallium can be mimicked by enhancing the exit rates from the open state. All of the other rate constants are constrained by the model. (B) Simulated currents for permeating potassium (black trace) and thallium (gray traces) reveal that the activation rate is altered by an increase in the rate from going to the open state to the flicker state. (C) Similarly, deactivation rates are decreased by the increase in the open to flicker rate in simulated currents for permeating potassium (black trace) and thallium (gray trace).

closing transitions. The gating mechanisms involving S6 motion and S4 motion are probably not significantly affected by the collapse of the selectivity filter.

Interestingly, rubidium consistently decreases the flicker in the single channel data for several potassium channels, including BK and KcsA (Demo and Yellen, 1992; Mienville and Clay, 1996, 1997; Pusch et al., 2000; Choe et al., 2001; LeMasurier et al., 2001). Rubidium has a different occupancy in the selectivity filter because of its larger size. It occupies three sites in the selectivity filter instead of four, with two of the sites in slightly different places than the potassium binding sites. Demo and Yellen (1992) have proposed that rubidium occupancy stabilizes the open state. It may be doing this by preventing the collapse of the selectivity filter by

TABLE III  
Scheme 3 Kinetic Parameters

Parameters	Permeating K <sup>+</sup>	Permeating Tl <sup>+</sup>	Parameters	Permeating K <sup>+</sup>	Permeating Tl <sup>+</sup>
	$s^{-1}$	$s^{-1}$		$s^{-1}$	$s^{-1}$
$\alpha(0)^a$	1110	1110	$k1^a$	500	3000
$\beta(0)$	32120	32120	$k2^a$	10000	10000
$\delta_0(0)^a$	0.0074	0.003	$k3^a$	1400	571
$\delta_1(0)^a$	0.126	0.0514	$k40^a$	0.00014	0.00014
$\delta_2(0)^a$	2.14	0.8743	$k41^a$	0.004	0.0024
$\delta_3(0)^a$	25.7	10.49	$k42^a$	0.0405	0.0405
$\delta_4(0)^a$	47.3	20.122	$k43^a$	0.688	0.688
$\gamma_0(0)$	3700	3700	$k44^a$	11.68	11.68
$\gamma_1(0)$	3700	3700	$z_\alpha$	+0.275 <i>e</i>	+0.275 <i>e</i>
$\gamma_2(0)$	3700	3700	$z_\beta$	-0.275 <i>e</i>	-0.275 <i>e</i>
$\gamma_3(0)$	2610	2610	$z_\delta$	+0.262 <i>e</i>	+0.262 <i>e</i>
$\gamma_4(0)$	295	295	$z_\gamma$	-0.138 <i>e</i>	-0.138 <i>e</i>

<sup>a</sup>These rate constants were sufficient to characterize the kinetic behavior of the model with the following additional parameters:  $D = 17$ ,  $f = \sqrt{D}$ ,  $L(0) = 8e^{-6} = \alpha/\beta$ ,  $V_{hc} = +150$  mV.

occupying the space between site two and three. This is exactly the site where Gly77 occludes the pore in the collapsed structure (Zhou and MacKinnon, 2003). The occupancy of thallium in the selectivity filter may be lower at that particular site, and would destabilize the conducting form of the selectivity filter.

Zhou and MacKinnon proposed that the high conduction rate of potassium channels is facilitated by the coupling of ion binding to a protein conformational change (Zhou and MacKinnon, 2003). It is well accepted that ionic repulsion between ions contributes to the high flux of the selective pore; this is supported by the fact that more than one potassium can bind in the selectivity filter at one time (Zhou et al., 2001; Zhou and MacKinnon, 2003). The conformational change undergone by the selectivity filter of KcsA may also enhance the conductance of the channel. If the energy required to stay in the conducting form comes from the free energy of ion binding, then permeating ions cannot bind as tightly, thus increasing conductance (Zhou et al., 2001). BK channels have the highest conductance of all potassium channels. If this mechanism is contributing to the high conduction rate of BK channels, then flicker would be a predicted side effect. In other words, it is possible that BK channels have a high conductance because of the two conformations in the selectivity filter. It has been demonstrated that electrostatic contributions from charged residues can contribute to the high conductance (Brelidze et al., 2003; Nimigean et al., 2003). However, even after these charges are neutralized, the conductance of these channels is still very large (Brelidze et al., 2003; Nimigean et al., 2003). Flicker closings are also seen in smaller-conductance channels such as *Shaker* (Hoshi et al., 1994); however, these events are not nearly as prevalent as they are in

larger conductance channels such as BK. Thus the large conductance of BK channels may be due to the combination of electrostatic effects and selectivity filter destabilization.

It has been reported that internal TEA induces the collapse of the KcsA selectivity filter presumptively by preventing the selectivity filter from being occupied by ions (Lenaeus et al., 2005). The authors of this work propose that the conformation change induced by TEA binding is the equivalent of the slow inactivation conformational change observed with many voltage-activated potassium channels (Lenaeus et al., 2005). Is it possible that slow-type inactivation and single-channel flicker are due to the same conformational change in the selectivity filter? Permeating ions and the occupancy of sites in the selectivity filter are known to alter the properties of C-type inactivation (Lopez-Barneo et al., 1993; Baukrowitz and Yellen, 1995, 1996; Harris et al., 1998; Ogielska and Aldrich, 1998; Fedida et al., 1999; Ogielska and Aldrich, 1999). Although BK channels do not undergo C-type inactivation, this is an intriguing hypothesis.

#### Conclusion

The effects of thallium on the gating of the BK channel reveal how possible conformational changes in the selectivity filter can effect the gating of the channel. With external thallium, these effects may be due to allosteric interactions with the voltage sensor. Permeating thallium was found to shift the activation curve and increase the flicker in single channel data. This may be caused by thallium stabilizing a collapsed state of the selectivity filter. The interaction between permeating ions and the collapsed state of the selectivity filter may be an important mechanism for conductance of BK channels.

We thank Sonja Pyott, Anthony Fodor, and Jon Sack for helpful comments on the manuscript. Frank Horrigan and Shalini Gera provided valuable experimental advice and discussion.

This work was supported by a predoctoral fellowship from the American Heart Association for R.A. Piskorowski. R.W. Aldrich is an investigator with the Howard Hughes Medical Institute.

Olaf S. Andersen served as editor.

Submitted: 30 December 2005

Accepted: 30 March 2006

## REFERENCES

- Barrett, J.N., K.L. Magleby, and B.S. Pallotta. 1982. Properties of single calcium-activated potassium channels in cultured rat muscle. *J. Physiol.* 331:211–230.
- Baukrowitz, T., and G. Yellen. 1995. Modulation of K<sup>+</sup> current by frequency and external [K<sup>+</sup>]: a tale of two inactivation mechanisms. *Neuron.* 15:951–960.
- Baukrowitz, T., and G. Yellen. 1996. Use-dependent blockers and exit rate of the last ion from the multi-ion pore of a K<sup>+</sup> channel. *Science.* 271:653–656.
- Blatz, A.L., and K.L. Magleby. 1984. Ion conductance and selectivity of single calcium-activated potassium channels in cultured rat muscle. *J. Gen. Physiol.* 84:1–23.
- Brelidze, T.I., X. Niu, and K.L. Magleby. 2003. A ring of eight conserved negatively charged amino acids doubles the conductance of BK channels and prevents inward rectification. *Proc. Natl. Acad. Sci. USA.* 100:9017–9022.
- Chen, F.S., D. Steele, and D. Fedida. 1997. Allosteric effects of permeating cations on gating currents during K<sup>+</sup> channel deactivation. *J. Gen. Physiol.* 110:87–100.
- Chepilkov, S., H. Zhou, H. Sackin, and L.G. Palmer. 1995. Permeation and gating properties of a cloned renal K<sup>+</sup> channel. *Am. J. Physiol.* 268:C389–C401.
- Choe, H., H. Sackin, and L.G. Palmer. 2001. Gating properties of inward-rectifier potassium channels: effects of permeant ions. *J. Membr. Biol.* 184:81–89.
- Clay, J.R., and M.F. Shlesinger. 1983. Effects of external cesium and rubidium on outward potassium currents in squid axons. *Biophys. J.* 42:43–53.
- Clay, J.R., and M.F. Shlesinger. 1984. Analysis of the effects of cesium ions on potassium channel currents in biological membranes. *J. Theor. Biol.* 107:189–201.
- Consiglio, J.F., P. Andalib, and S.J. Korn. 2003. Influence of pore residues on permeation properties in the Kv2.1 potassium channel. Evidence for a selective functional interaction of K<sup>+</sup> with the outer vestibule. *J. Gen. Physiol.* 121:111–124.
- Consiglio, J.F., and S.J. Korn. 2004. Influence of permeant ions on voltage sensor function in the Kv2.1 potassium channel. *J. Gen. Physiol.* 123:387–400.
- Cox, D.H., J. Cui, and R.W. Aldrich. 1997. Allosteric gating of a large conductance Ca-activated K<sup>+</sup> channel. *J. Gen. Physiol.* 110:257–281.
- Cui, J., D.H. Cox, and R.W. Aldrich. 1997. Intrinsic voltage dependence and Ca<sup>2+</sup> regulation of mslo large conductance Ca-activated K<sup>+</sup> channels. *J. Gen. Physiol.* 109:647–673.
- Demo, S.D., and G. Yellen. 1992. Ion effects on gating of the Ca<sup>2+</sup>-activated K<sup>+</sup> channel correlate with occupancy of the pore. *Biophys. J.* 61:639–648.
- Fedida, D., N.D. Maruoka, and S. Lin. 1999. Modulation of slow inactivation in human cardiac Kv1.5 channels by extra- and intracellular permeant cations. *J. Physiol.* 515(Pt 2):315–329.
- Gomez-Lagunas, F. 1997. *Shaker* B K<sup>+</sup> conductance in Na<sup>+</sup> solutions lacking K<sup>+</sup> ions: a remarkably stable non-conducting state produced by membrane depolarizations. *J. Physiol.* 499(Pt 1):3–15.
- Harris, R.E., H.P. Larsson, and E.Y. Isacoff. 1998. A permanent ion binding site located between two gates of the *Shaker* K<sup>+</sup> channel. *Biophys. J.* 74:1808–1820.
- Haug, T., R. Olcese, L. Toro, and E. Stefani. 2004a. Regulation of K<sup>+</sup> flow by a ring of negative charges in the outer pore of BKCa channels. Part II: Neutralization of aspartate 292 reduces long channel openings and gating current slow component. *J. Gen. Physiol.* 124:185–197.
- Haug, T., D. Sigg, S. Ciani, L. Toro, E. Stefani, and R. Olcese. 2004b. Regulation of K<sup>+</sup> flow by a ring of negative charges in the outer pore of BKCa channels. Part I: Aspartate 292 modulates K<sup>+</sup> conduction by external surface charge effect. *J. Gen. Physiol.* 124:173–184.
- Hille, B. 2001. Ion channels of excitable membranes. Volume 3. Sinauer Associates, Inc., Sunderland, MA. 814 pp.
- Horrigan, F.T., and R.W. Aldrich. 1999. Allosteric voltage gating of potassium channels II. Mslo channel gating charge movement in the absence of Ca<sup>2+</sup>. *J. Gen. Physiol.* 114:305–336.
- Horrigan, F.T., and R.W. Aldrich. 2002. Coupling between voltage sensor activation, Ca<sup>2+</sup> binding and channel opening in large conductance (BK) potassium channels. *J. Gen. Physiol.* 120:267–305.
- Horrigan, F.T., J. Cui, and R.W. Aldrich. 1999. Allosteric voltage gating of potassium channels I. Mslo ionic currents in the absence of Ca<sup>2+</sup>. *J. Gen. Physiol.* 114:277–304.
- Hoshi, T., W.N. Zagotta, and R.W. Aldrich. 1994. *Shaker* potassium channel gating. I: Transitions near the open state. *J. Gen. Physiol.* 103:249–278.
- Hurst, R.S., M.J. Roux, L. Toro, and E. Stefani. 1997. External barium influences the gating charge movement of *Shaker* potassium channels. *Biophys. J.* 72:77–84.
- Kiss, L., and S.J. Korn. 1998. Modulation of C-type inactivation by K<sup>+</sup> at the potassium channel selectivity filter. *Biophys. J.* 74:1840–1849.
- Kiss, L., J. LoTurco, and S.J. Korn. 1999. Contribution of the selectivity filter to inactivation in potassium channels. *Biophys. J.* 76:253–263.
- Lagrutta, A.A., K.Z. Shen, A. Rivard, R.A. North, and J.P. Adelman. 1998. Aromatic residues affecting permeation and gating in dSlo BK channels. *Pflugers Arch.* 435:731–739.
- LeMasurier, M., L. Heginbotham, and C. Miller. 2001. KcsA: it's a potassium channel. *J. Gen. Physiol.* 118:303–314.
- Lenaeus, M.J., M. Vamvouka, P.J. Focia, and A. Gross. 2005. Structural basis of TEA blockade in a model potassium channel. *Nat. Struct. Mol. Biol.* 12:454–459.
- Lippiat, J.D., N.B. Standen, and N.W. Davies. 1998. Block of cloned BKCa channels (rSlo) expressed in HEK 293 cells by N-methyl D-glucamine. *Pflugers Arch.* 436:810–812.
- Loboda, A., A. Melishchuk, and C. Armstrong. 2001. Dilated and de-funct K channels in the absence of K<sup>+</sup>. *Biophys. J.* 80:2704–2714.
- Long, S.B., E.B. Campbell, and R. Mackinnon. 2005a. Crystal structure of a mammalian voltage-dependent *Shaker* family K<sup>+</sup> channel. *Science.* 309:897–903.
- Long, S.B., E.B. Campbell, and R. Mackinnon. 2005b. Voltage sensor of Kv1.2: structural basis of electromechanical coupling. *Science.* 309:903–908.
- Lopez-Barneo, J., T. Hoshi, S.H. Heinemann, and R.W. Aldrich. 1993. Effects of external cations and mutations in the pore region on C-type inactivation of *Shaker* potassium channels. *Receptors Channels.* 1:61–71.
- Lu, T., A.Y. Ting, J. Mainland, L.Y. Jan, P.G. Schultz, and J. Yang. 2001a. Probing ion permeation and gating in a K<sup>+</sup> channel with backbone mutations in the selectivity filter. *Nat. Neurosci.* 4:239–246.
- Lu, T., L. Wu, J. Xiao, and J. Yang. 2001b. Permeant ion-dependent changes in gating of Kir2.1 inward rectifier potassium channels. *J. Gen. Physiol.* 118:509–522.

- Magleby, K.L., and B.S. Pallotta. 1983. Burst kinetics of single calcium-activated potassium channels in cultured rat muscle. *J. Physiol.* 344:605–623.
- Matteson, D.R., and R.P. Swenson Jr. 1986. External monovalent cations that impede the closing of K channels. *J. Gen. Physiol.* 87:795–816.
- McManus, O.B., and K.L. Magleby. 1988. Kinetic states and modes of single large-conductance calcium-activated potassium channels in cultured rat skeletal muscle. *J. Physiol.* 402:79–120.
- McManus, O.B., and K.L. Magleby. 1991. Accounting for the Ca<sup>2+</sup>-dependent kinetics of single large-conductance Ca<sup>2+</sup>-activated K<sup>+</sup> channels in rat skeletal muscle. *J. Physiol.* 443:739–777.
- Melishchuk, A., A. Loboda, and C.M. Armstrong. 1998. Loss of *Shaker* K channel conductance in 0 K<sup>+</sup> solutions: role of the voltage sensor. *Biophys. J.* 75:1828–1835.
- Mienville, J.M., and J.R. Clay. 1996. Effects of intracellular K<sup>+</sup> and Rb<sup>+</sup> on gating of embryonic rat telencephalon Ca<sup>2+</sup>-activated K<sup>+</sup> channels. *Biophys. J.* 70:778–785.
- Mienville, J.M., and J.R. Clay. 1997. Ion conductance of the Ca<sup>2+</sup>-activated maxi-K<sup>+</sup> channel from the embryonic rat brain. *Biophys. J.* 72:188–192.
- Neyton, J., and C. Miller. 1988a. Discrete Ba<sup>2+</sup> block as a probe of ion occupancy and pore structure in the high-conductance Ca<sup>2+</sup>-activated K<sup>+</sup> channel. *J. Gen. Physiol.* 92:569–586.
- Neyton, J., and C. Miller. 1988b. Potassium blocks barium permeation through a calcium-activated potassium channel. *J. Gen. Physiol.* 92:549–567.
- Neyton, J., and M. Pelleschi. 1991. Multi-ion occupancy alters gating in high-conductance, Ca<sup>2+</sup>-activated K<sup>+</sup> channels. *J. Gen. Physiol.* 97:641–665.
- Nimigeon, C.M., J.S. Chappie, and C. Miller. 2003. Electrostatic tuning of ion conductance in potassium channels. *Biochemistry.* 42:9263–9268.
- Nimigeon, C.M., and K.L. Magleby. 2000. Functional coupling of the  $\beta 1$  subunit to the large conductance Ca<sup>2+</sup>-activated K<sup>+</sup> channel in the absence of Ca<sup>2+</sup>. Increased Ca<sup>2+</sup> sensitivity from a Ca<sup>2+</sup>-independent mechanism. *J. Gen. Physiol.* 115:719–736.
- Ogielska, E.M., and R.W. Aldrich. 1998. A mutation in S6 of *Shaker* potassium channels decreases the K<sup>+</sup> affinity of an ion binding site revealing ion-ion interactions in the pore. *J. Gen. Physiol.* 112:243–257.
- Ogielska, E.M., and R.W. Aldrich. 1999. Functional consequences of a decreased potassium affinity in a potassium channel pore. Ion interactions and C-type inactivation. *J. Gen. Physiol.* 113:347–358.
- Pusch, M., L. Bertorello, and F. Conti. 2000. Gating and flickery block differentially affected by rubidium in homomeric KCNQ1 and heteromeric KCNQ1/KCNE1 potassium channels. *Biophys. J.* 78:211–226.
- Rothberg, B.S., and K.L. Magleby. 1998. Kinetic structure of large-conductance Ca<sup>2+</sup>-activated K<sup>+</sup> channels suggests that the gating includes transitions through intermediate or secondary states. A mechanism for flickers. *J. Gen. Physiol.* 111:751–780.
- Rothberg, B.S., and K.L. Magleby. 1999. Gating kinetics of single large-conductance Ca<sup>2+</sup>-activated K<sup>+</sup> channels in high Ca<sup>2+</sup> suggest a two-tiered allosteric gating mechanism. *J. Gen. Physiol.* 114:93–124.
- Rothberg, B.S., and K.L. Magleby. 2000. Voltage and Ca<sup>2+</sup> activation of single large-conductance Ca<sup>2+</sup>-activated K<sup>+</sup> channels described by a two-tiered allosteric gating mechanism. *J. Gen. Physiol.* 116:75–99.
- Swenson, R.P., Jr., and C.M. Armstrong. 1981. K<sup>+</sup> channels close more slowly in the presence of external K<sup>+</sup> and Rb<sup>+</sup>. *Nature.* 291:427–429.
- Talukder, G., and R.W. Aldrich. 2000. Complex voltage-dependent behavior of single unliganded calcium-sensitive potassium channels. *Biophys. J.* 78:761–772.
- Wang, Z., X. Zhang, and D. Fedida. 1999. Gating current studies reveal both intra- and extracellular cation modulation of K<sup>+</sup> channel deactivation. *J. Physiol.* 515(Pt 2):331–339.
- Wu, Y.C., J.J. Art, M.B. Goodman, and R. Fettiplace. 1995. A kinetic description of the calcium-activated potassium channel and its application to electrical tuning of hair cells. *Prog. Biophys. Mol. Biol.* 63:131–158.
- Zheng, J., and F.J. Sigworth. 1998. Intermediate conductances during deactivation of heteromultimeric *Shaker* potassium channels. *J. Gen. Physiol.* 112:457–474.
- Zhou, Y., and R. MacKinnon. 2003. The occupancy of ions in the K<sup>+</sup> selectivity filter: charge balance and coupling of ion binding to a protein conformational change underlie high conduction rates. *J. Mol. Biol.* 333:965–975.
- Zhou, Y., J.H. Morais-Cabral, A. Kaufman, and R. MacKinnon. 2001. Chemistry of ion coordination and hydration revealed by a K<sup>+</sup> channel-Fab complex at 2.0 Å resolution. *Nature.* 414:43–48.